

12

LEVEL II

AD A 109 490

Project Report

DCA-16

R.P. Rafuse

Effects of Sandstorms and Explosion-Generated Atmospheric Dust on Radio Propagation

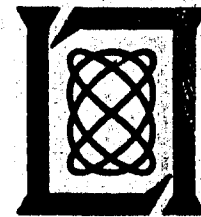
10 November 1981

Prepared for the Defense Communications Agency under Electronic Systems Division Contract F19628-80-C-0002 by

Lincoln Laboratory

MASSACHUSETTS INSTITUTE OF TECHNOLOGY

LEXINGTON, MASSACHUSETTS



Approved for public release; distribution unlimited.

DTIC ELECTE  
JAN 1 1 1982  
S B

FILE COPY

The work reported in this document was performed at Lincoln Laboratory, a center for research operated by Massachusetts Institute of Technology. This work was sponsored by the Military Satellite Communications Systems Office of the Defense Communications Agency under Air Force Contract F19628-80-C-0002.

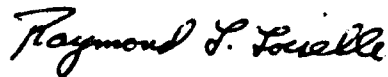
This report may be reproduced to satisfy needs of U.S. Government agencies.

The views and conclusions contained in this document are those of the contractor and should not be interpreted as necessarily representing the official policies, either expressed or implied, of the United States Government.

The Public Affairs Office has reviewed this report, and it is releasable to the National Technical Information Service, where it will be available to the general public, including foreign nationals.

This technical report has been reviewed and is approved for publication.

FOR THE COMMANDER



Raymond L. Loiselle, Lt.Col., USAF  
Chief, ESD Lincoln Laboratory Project Office

MASSACHUSETTS INSTITUTE OF TECHNOLOGY  
LINCOLN LABORATORY

**EFFECTS OF SANDSTORMS AND EXPLOSION-GENERATED  
ATMOSPHERIC DUST ON RADIO PROPAGATION**

*R.P. RAFUSE*  
*Group 61*

PROJECT REPORT DCA-16

10 NOVEMBER 1981

DTIC  
ELECTE  
JAN 1 1 1982  
B

Approved for public release; distribution unlimited.

LEXINGTON

MASSACHUSETTS

*i/11*

ABSTRACT

Suspended particulate matter in the atmosphere, generated by natural phenomena such as dust and sandstorms or by man-made near-surface explosions, has been suspected as a cause of microwave and millimeter-wave communications systems outages. An analysis carried out on the radio-frequency and optical effects of such dust clouds and the results, coupled with available information on particle-size distributions and suspended mass, indicates that the radio-frequency effects should be essentially negligible. However, observed changes in the atmospheric pressure, temperature, and humidity which accompany dust storms (and explosions) can account for all of the observed effects on microwave links. With the exception of water entrained in large explosions, most such effects are, however, virtually frequency-independent; therefore, dust-storm activity and clouds raised by detonations should not be considered a threat peculiar to EHF SATCOM or other millimeter-wave based communications systems.

Accession No.	
1	✓
2	
3	
4	
5	
6	
7	
8	
9	
10	
11	
12	
13	
14	
15	
16	
17	
18	
19	
20	
21	
22	
23	
24	
25	
26	
27	
28	
29	
30	
31	
32	
33	
34	
35	
36	
37	
38	
39	
40	
41	
42	
43	
44	
45	
46	
47	
48	
49	
50	
51	
52	
53	
54	
55	
56	
57	
58	
59	
60	
61	
62	
63	
64	
65	
66	
67	
68	
69	
70	
71	
72	
73	
74	
75	
76	
77	
78	
79	
80	
81	
82	
83	
84	
85	
86	
87	
88	
89	
90	
91	
92	
93	
94	
95	
96	
97	
98	
99	
100	

## TABLE OF CONTENTS

Abstract	iii
List of Illustrations	vi
List of Tables	vii
I. INTRODUCTION	1
1.1 Rationale	1
1.2 Report Description	1
1.3 Major Conclusions	2
II. ANALYSIS	4
2.1 Introduction	4
2.2 Optical-Wavelength Attenuations: Visibility and Meteorological Range	5
2.3 Radio-Frequency Effects: Attenuation and Phase Shift	6
2.4 Event Morphology: Particle-Size Distributions and Suspended Mass	8
2.4.1 Introduction	8
2.4.2 Sandstorms and Dust Storms	13
2.4.3 Conventional and Nuclear Explosions	19
2.4.3.1 Nuclear Explosions	19
2.4.3.2 Conventional Explosions	32
2.4.4 Comparisons	32
2.5 Material Constants	35
2.6 Comparison of Fog and Dust	37
2.7 The Forgotten Parameter: Changes in Atmospheric Refractive Index Not Connected With Dust Content	41
III. CONCLUDING REMARKS	52
Acknowledgments	54
References	55

## LIST OF ILLUSTRATIONS

2.4.1.1	Terminal velocities of small spherical particles falling in still air at sea level.	12
2.4.2.1	Measured and extrapolated particle-size distributions for light-wind, medium-wind and sandstorm conditions at Camp Derj in the Libyan Sahara.	15
2.4.2.2	Probability density distributions for particle radii as determined from the data in Fig. 2.4.2.1.	16
2.4.2.3	Diurnal probability of occurrence of blowing dust and dust storms in Kuwait.	20
2.4.2.4	Yearly probability of occurrence of blowing dust and dust storms in Kuwait.	21
2.4.2.5	Cumulative probability density distribution function for the duration of blowing-dust occurrences and dust storms.	22
2.4.3.1	Normalized pedestal radius and height versus normalized burst height.	25
2.4.3.2	Normalized pedestal dust density versus normalized burst height.	26
2.4.3.3	Stem-region suspended mass density as a function of time for a 100-kt detonation at 100-meter altitude.	28
2.4.4.1	Radial probability density distributions for nuclear detonations over two soil extremes and a sandstorm.	33
2.7.1	Vertical structure of the advancing lobe of a haboob given with the height, $H$ , and distance into the lobe, $D$ , normalized with respect to the maximum lobe height, $H_{\max}$ (typically 1000 to 2000 m).	44

## LIST OF TABLES

2.4.1.1	Sand- and Dust-Storm Parameters as a Function of Wind State	18
2.4.3.1	Dust Formation Characteristics of a Nuclear Detonation as a Function of Normalized Burst Altitude	24
2.4.3.2	Stem and Pedestal Dust Parameters for a 100-kt Detonation over Cohesive Soil at an Altitude of 100 meters	31
2.4.4.1	Comparison of Effective Radius, $r_e$ , Suspended Mass, $W$ , and Meteorological Range, $R_m$ , for Nuclear Detonations over Two Soil Extremes and a Sandstorm	34
2.6.1	Temperature Dependence of the Constants in the Debye Formulation of (2.6.2)	39
2.6.2	Comparison of Worst-Case Fog and Dust Excess Phase and Attenuation at 11 and 44 GHz.	42
2.7.1	External and Internal Characteristics of a Haboob or Dust Storm	47
2.7.2	Indices of Refraction, Path Losses Due to $O_2$ and $H_2$ , and Visibility External to and Internal to a Haboob	48
2.7.3	Comparisons of Density Changes and 11- and 44-GHz Excess Phase Shift and Attenuation Changes from Inside and Outside the Arizona Haboob	49

## I. INTRODUCTION

### 1.1 Rationale

In recent years there has been increased interest in the effects of dust on millimeter-wave communications. In part this interest is the result of the move towards 30/20 and 44/20 GHz as uplink/downlink frequency assignments for MILSATCOM systems and the recognition that attenuation and phase-shift produced by small suspended dielectric particles increases directly with frequency. Also, measurements of propagation near ground-zero in simulated nuclear explosions [Burns and Crawley, 1979] and measurements on an 11-GHz terrestrial link in Iraq [Al-Hafid, Gupta, and Buni, 1979; Al-Hafid, Gupta and Ibrahim, 1980] seemed to indicate a pronounced effect on propagation loss by a sandstorm located along the path or by the particulate matter and dust raised by an explosion. In addition, other observations on microwave communications outages during sandstorms in the Middle East have been made by US civilian and military communicators.

Any attempt to model the effects of suspended particulate matter on millimeter-wave communications must estimate the particle-size distributions, suspended-mass densities and dielectric properties of the particles. Fortunately, there is enough empirical evidence gathered in the literature so that reasonable bounds on each of the parameters can be obtained. From these studies a good estimate of the loss and excess phase shift due to natural events, such as sand and dust storms, or man-made events, such as nuclear explosions, can be made. In addition, other concurrent meteorological parameters which can affect radio propagation should be examined.

### 1.2 Report Description

Sections 2.2 and 2.3 analyze the optical and radio-frequency behaviors of suspended particulate matter. The following section, 2.4, discusses the gross morphology of dust storms and dust raised by large explosions and presents the necessary statistical analyses of particle sizes and numbers. From these



parameters and material-constant results from Section 2.5, theoretical values for both optical and radio-frequency behaviors of dust clouds can be obtained. Because water vapor often condenses on the smallest nuclei in dust clouds raised by large explosions and, at times, on dust raised in dust storms, the comparison between fog and dust given in Section 2.6 seems appropriate. Finally, in Section 2.7 the effects on propagation of the other meteorological phenomena which accompany dust storms (and nuclear detonations) are analyzed. Section III presents the conclusions and recommendations that result from this study; the major conclusions are detailed in the next section (Section 1.3).

### 1.3 Major Conclusions

The literature on the effects of suspended atmospheric particulate matter on radio propagation is sparse and confusing. However, "after the dust has settled"\* several facts stand out clearly. They are

- a. Dust is a convenient "tracer" for convective storms and allows the time and space structure of the differential air masses to be examined in detail.
- b. Large explosions near the surface, either nuclear or conventional, raise dust clouds which rapidly decay in density (in 10 seconds or so) to densities of the same order, or perhaps slightly greater, as those seen in severe sandstorms or dust storms. Multiple detonations would probably increase the total dust density somewhat; coupled with an increase in total RF path filled with dust, multiple-event scenarios might result in as much as an order of magnitude increase in effects of dust.
- c. A careful examination of the visual and rf properties of the entrained dust in severe dust storms cannot uncover any effect, even at as high a frequency as 44 GHz, other than a minor (0.04 dB/km) increase in path

---

\*The reader must please forgive the author; the temptation was too great to resist.

attenuation. It is unlikely that late-time dust densities entrained by a nuclear detonation or detonations will be more than an order-of-magnitude greater than a severe dust storm; if so, the effects of such dust on radio propagation will be minimal.

d. The observed propagation effects, which include path attenuation and fading, noted during a sandstorm can be entirely accounted for by the refractive index changes brought about by the temperature and humidity changes and turbulence accompanying the storm.

e. Except for the first 10's of seconds on rf paths that traverse near ground-zero, the dust entrained in large explosions, either nuclear or conventional, will probably not have a significant effect on propagation even at millimeter-wave frequencies. However, the changes in density of the air caused by the thermal properties of the explosion will be several orders-of-magnitude greater than the density of entrained dust. Such density changes, coupled with water-droplet nucleation in the cloud and associated turbulence, will be the primary contributors to propagation disturbances following large explosions.

f. The atmospheric refractive index changes due to temperature are essentially frequency independent. Although the relative humidity changes markedly during a sandstorm, the total water content does not. Consequently, in a dust storm environment whatever effects are present at low microwave frequencies will not be exacerbated by a move to millimeter-wave frequencies.

g. For large explosions over dry soil the major propagation effects will be caused by the large changes in density of the air due to temperature changes. Such effects should, therefore, be relatively frequency independent. If the explosion takes place on a water surface, the entrained water can be a significant attenuator, with an absorption (in dB/km) increasing roughly as the square of the frequency. Little data seems to be available, however, on the expected density of entrained water in such cases. Rain, formed by nucleation on the high-altitude dust cloud will also cause absorption and scattering at millimeter-wave frequencies.

## II. ANALYSIS

### 2.1 INTRODUCTION

The estimation of optical and radio-frequency properties of dust clouds is complicated by the fact that the particle sizes are characterized by random distributions of radii varying over several orders of magnitude. Consequently, the cross-sectional areas and volumes are measured by the expectations of the squares and cubes of the radius,  $\overline{r^2}$  and  $\overline{r^3}$ , respectively. The determination of such factors requires knowledge of the probability density distribution for the particle radius. Even the word "radius" is used in a statistical sense, since most dust particles are by no means perfect spheres. In fact, various "rules-of-thumb" have been developed to scale from the mesh size of separation screens to equivalent radii [Bagnold, 1941], with the equivalent radii being somewhat less (~30%) than the screen spacing. Similar corrections are necessary for size data obtained by optical and electron microscopy.

Once the particle-size distributions are known, the scattering and absorption properties must be determined. Exact solutions are impossible for irregularly-shaped particles except in the limit where the wavelength of the incident radiation is much larger than the average circumference of the particle. If all particles are assumed to be perfectly spherical, the Mie scattering formulation can be used [Stratton, 1941]. For particles large compared to the wavelength, simple optical-blockage calculations are adequate; for particles small compared to wavelength, Rayleigh scattering can be assumed. In the intermediate size range, difficult and involved computations, with computer simulation, must be carried out.

In the following sections, in the interests of simplicity, Rayleigh scattering will be assumed to hold for all particle sizes at radio frequencies and simple optics will hold for all particle sizes at optical wavelengths. In most cases the errors produced by such assumptions will be small. Probably the only cases where significant error might exist in the radio-frequency

model would be in the early time histories at low altitudes in the dust clouds produced by man-made nuclear or conventional explosions or such natural events as volcanic eruptions. Such large particles generally have brief lives, however, because updraft winds do not have sufficient velocity to keep them suspended once their explosively derived energies are expended.

## 2.2 Optical-Wavelength Attenuations: Visibility and Meteorological Range

If the wavelength of the incident radiation is such that  $\lambda \ll 2\pi r$  over the range of particle radii,  $r$ , then the attenuation coefficient becomes

$$\alpha = 2N_T \pi \overline{r^2} \quad \text{m}^{-1} \quad (2.2.1)$$

where  $N_T$  is the total count of particles/ $\text{m}^3$  and  $\overline{r^2}$  is the mean-square radius. The intensity versus distance,  $R$ , will become

$$I(R) = I(0)e^{-\alpha R} \quad (2.2.2)$$

[Middleton, 1952]. The classical definition of meteorological range occurs for a liminal contrast of 0.02, so

$$R_m = \frac{1}{\alpha} \ln \frac{1}{0.02} = \frac{3.912}{\alpha} \quad \text{m} \quad (2.2.3)$$

Although there have been arguments raised for somewhat different values of liminal contrast [see Middleton, 1952], in particular 0.031, in the following sections the value used in (2.2.3) will be chosen. Using (2.2.1) in (2.2.3)

$$R_m = \frac{0.623}{N_T \overline{r^2}} \quad \text{m} \quad (2.2.4)$$

The total material suspended in  $\text{kg}/\text{m}^3$  is given by

$$W = N_T \frac{4}{3} \pi \overline{r^3} \sigma \quad \text{kg}/\text{m}^3 \quad (2.2.5)$$

where  $\sigma$  is the density of the individual particles in  $\text{kg/m}^3$ .

Substituting (2.2.5) in (2.2.1) gives the attenuation coefficient as

$$\alpha = \frac{3}{2} \frac{W}{\sigma} \frac{1}{r_e} \text{ m}^{-1} \quad (2.2.6)$$

where the equivalent radius,  $r_e$ , is defined as

$$r_e = \frac{r^3}{r^2} \text{ m} \quad (2.2.7)$$

It is interesting to note that  $W/\sigma$  represents the fraction of the atmospheric volume filled by particles and can be written in terms of  $r_e$  and  $R_m$ , using (2.2.6) and (2.2.3), as

$$\eta = W/\sigma = 2.608 \frac{r_e}{R_m} \quad (2.2.8)$$

From (2.2.3) and (2.2.6), it becomes clear why smokes are much more effective than dusts at reducing visual range. The range can be written as

$$R_m = 2.608 r_e \left( \frac{\sigma}{W} \right) \text{ m} \quad (2.2.9)$$

Chemical smokes have values of  $r_e$  one or more orders of magnitude smaller than dusts, so much smaller amounts (in  $W/\sigma$ ) of smoke than dust can produce equivalent losses in visual range.

### 2.3 Radio-Frequency Effects - Attenuation and Phase Shift

Since very few long-lived dust particles will approach  $10^{-3}$  m in radius, for frequencies up to 44 GHz there will be little error in assuming Rayleigh scattering. Some authors [for example, Thompson, 1978] have gone so far as to solve the Mie scattering formulation for the entire particle size range including the case where  $\lambda \sim 2\pi r$ . In the analysis to follow, classical Rayleigh scattering will be assumed.

For Rayleigh scattering [see Stratton, 1941, McCartney, 1976; and/or Van DeHulst, 1957] the effective refractive index of the scattering medium becomes

$$n = 1 - j \overline{S(0)} 2\pi N_T k^3 \quad (2.3.1)$$

where  $k=2\pi/\lambda$  and  $\overline{S(0)}$  is the average forward scattering function:

$$\overline{S(0)} = jk^3 \left( \frac{\epsilon-1}{\epsilon+2} \right) r^3 \quad (2.3.2)$$

at the frequencies of interest. It is assumed that the particles are non-magnetic ( $\mu=\mu_0$ ) and have the complex relative dielectric constant

$$\epsilon = \epsilon' - j\epsilon'' = \epsilon' [1 - j \tan \delta] \quad (2.3.3)$$

Therefore, with (2.3.2) in (2.3.1)

$$n = 1 + 2\pi N_T \left( \frac{\epsilon-1}{\epsilon+2} \right) r^3 \quad (2.3.4)$$

As in Section 2.2, the total suspended particulate mass  $W$ , given by (2.2.5), can be rearranged and substituted in (2.3.4) to obtain

$$n = 1 + \frac{3}{2} \frac{W}{\sigma} \left( \frac{\epsilon-1}{\epsilon+2} \right) \quad (2.3.5)$$

Note that  $W/\sigma$  represents the fraction of the volume filled by the dust particles. The E-field propagates as  $e^{-jk n R/R}$ ; therefore, removing the free-space behavior leaves an "excess" behavior characterized by  $\exp\{-jk(n-1)r\}$ . Consequently, the excess phase shift and attenuation can be written, respectively, as

$$k[\text{Re}\{n-1\}] = k \frac{3}{2} \frac{W}{\sigma} \text{Re} \left\{ \frac{\epsilon-1}{\epsilon+2} \right\} \text{ radians/m} \quad (2.3.6)$$

and

$$-K [\text{Im}\{n\}] = -k \frac{3}{2} \frac{W}{\sigma} \text{Im} \left\{ \frac{\epsilon-1}{\epsilon+2} \right\} \text{ nepers/m} \quad (2.3.7)$$

These relations are identical to those derived by Chu [1979]. Expressed in another fashion, (2.3.6) and (2.3.7) become, respectively,

$$\Delta\theta = 1800f_{\text{GHz}} \frac{W}{\sigma} \text{Re} \left\{ \frac{\epsilon-1}{\epsilon+2} \right\} \text{ }^\circ/\text{m} \quad (2.3.8)$$

and

$$L = -273f_{\text{GHz}} \frac{W}{\sigma} \text{Im} \left\{ \frac{\epsilon-1}{\epsilon+2} \right\} \text{ dB/m} \quad (2.3.9)$$

where  $f_{\text{GHz}}$  is the operating frequency expressed in GHz.

It is often useful to express the excess phase shift and attenuation in terms of observables such as visible range. From (2.2.8), the relations in (2.3.8) and (2.3.9) can be written as

$$\Delta\theta = 4.69 \times 10^6 f_{\text{GHz}} \frac{r_e}{R_m} \text{Re} \left\{ \frac{\epsilon-1}{\epsilon+2} \right\} \text{ }^\circ/\text{km} \quad (2.3.10)$$

$$L = -7.12 \times 10^5 f_{\text{GHz}} \frac{r_e}{R_m} \text{Im} \left\{ \frac{\epsilon-1}{\epsilon+2} \right\} \text{ dB/km} \quad (2.3.11)$$

Therefore, if the meteorological range in a dust or sandstorm is known, together with the equivalent radius of the particle-size distribution and the complex relative dielectric constant of the materials constituting the particles, the rf path properties can be directly inferred.

## 2.4 Event Morphology: Particle-Size Distributions and Suspended Mass

### 2.4.1 Introduction

Aerosol dispersions in the atmosphere, either natural (sand or dust storms) or man-made (debris and dust swept up and dispersed in a conventional

or nuclear explosion), have a statistical distribution of particle sizes. The particle size distribution is often plotted as  $dN/d\log_{10}r$  per  $m^3$  against the particle radius,  $r$ , in meters [Junge, 1957; Cadle, 1966], where  $N(r)$  is the number density of particles/ $m^3$ . An analysis of the scattering properties of these aerosols requires a knowledge of the first few moments of  $p(r)$ , the probability density distribution of the particle radius (in particular,  $\overline{r^2}$  and  $\overline{r^3}$ ).

If  $f(r)$  is written as

$$f(r) = dN/d\log_{10}r \quad m^{-3} \quad (2.4.1.1)$$

then

$$f(r) = dN/0.4343 \, d\ln r \quad m^{-3} \quad (2.4.1.2)$$

which can be rearranged as

$$dN = 0.4343 \frac{f(r)}{r} dr \quad m^{-3} \quad (2.4.1.3)$$

If  $f(r)$  is measured by sampling techniques over a range of particle sizes  $r_1 < r < r_2$ , the total number of particles within that range becomes

$$N_T = 0.4343 \int_{r_1}^{r_2} \frac{f(r)}{r} dr \quad m^{-3} \quad (2.4.1.4)$$

The probability density distribution of the particle radius then becomes

$$p(r) = \frac{1}{N_T} \frac{dN}{dr} = \frac{0.4343}{N_T} \frac{f(r)}{r} \quad m^{-1} \quad (2.4.1.5)$$

and the moments are

$$\overline{r^k} = \int_{r_1}^{r_2} r^k p(r) dr = \frac{0.4343}{N_T} \int_{r_1}^{r_2} r^{k-1} f(r) dr \quad m^k \quad (2.4.1.6)$$



In many cases, solid-particle dispersions are characterized over two or more decades of particle radius by

$$f(r) = cr^{-\nu} \quad m^{-3} \quad (2.4.1.7)$$

with  $3 < \nu < 4$  (in comparison, many fogs are characterized by  $\nu \approx 2$  [McCartney, 1976]). One is tempted to assume for teleological reasons that natural particles sizes should be log-normally distributed. In fact, Green and Lane [1957] have suggested that the log-normal distribution is "adequate" for dusts. However, over the entire aerosol size range the distribution is much more complex [Junge, 1957]. Measurements on sand-grain size by Bagnold [1941] indicate a number distribution varying as  $r^p$  for  $r < 0.3$  to  $0.5$  mm and  $r^q$  for  $r > 0.3$  to  $0.5$  mm, with  $p$  and  $q$  varying more or less independently over the range from 3 to 10.

Experimental particle-size data plotted as  $dN/d\log_{10}r$  versus  $\log_{10}r$  is relatively easy to analyze. The number of particles between two radii,  $r_1$  and  $r_2$ , can be obtained by multiplying the value of  $dN/d\log_{10}r$  for  $r = \sqrt{r_1 r_2}$  by the difference between the log radii,  $\log_{10}r_2 - \log_{10}r_1$  or  $\log_{10}(r_2/r_1)$ . That is,

$$\Delta N_{12} = \left\{ \left[ \frac{dN}{d\log_{10}r} \right]_{r=\sqrt{r_1 r_2}} \right\} \log_{10} r_2/r_1 \quad m^{-3} \quad (2.4.1.8)$$

The empirical data can then be broken up into  $K$  small segments and  $N_T$  obtained as

$$N_T = \sum_{\ell=1}^K \Delta N_{\ell, \ell+1} \quad m^{-3} \quad (2.4.1.9)$$

With  $dr = r_{\ell+1} - r_{\ell}$ , the probability density distribution for the radius can then be obtained, using (2.4.1.5), as a series of points

$$P_{\ell}(r) = \frac{1}{N_T} \frac{\Delta N_{\ell, \ell+1}}{r_{\ell+1} - r_{\ell}} \quad m^{-1} \quad (2.4.1.10)$$

and the moments obtained as

$$\overline{r^k} = \sum_{\ell=1}^K \hat{r}_{\ell}^k \frac{\Delta N_{\ell, \ell+1}}{N_T} \quad m^k \quad (2.4.1.11)$$

where  $\hat{r}_{\ell} = \sqrt{r_{\ell+1} r_{\ell}}$ .

Particles injected into the atmosphere by any mechanism will remain aloft indefinitely only if the vertical component of the winds is sufficient to override the terminal fall velocity of the particle. From Stokes Law and the physics of aerodynamic drag, the terminal velocity of spherical particles in air can be obtained [Green and Lane, 1957]. This terminal velocity and consequent time to fall 1 km (at sea level) is shown in Fig. 2.4.1.1. It should be noted that the terminal velocity for small particles at higher altitudes will be much higher than the sea-level values [Cadle, 1966].

Since the general "rule-of-thumb" gives a lofting or vertical wind velocity averaging about 1/5 of the horizontal value [Bagnold, 1941], surface winds of 180 km/hr (113 mph) are required to give a vertical component of 10 m/sec and support and loft particles up to  $10^{-3}$  m in radius. More reasonable values of surface winds in stormy conditions are in the order of 45 mph or 72 km/hr. For this value of surface wind velocity the lofting velocity would be about 4 m/sec and the maximum particle size observed would be about  $2 \times 10^{-4}$  m (0.2 mm). In fact, this maximum value is very close to that observed in desert dust storms [Schütz and Jaenicke, 1974; Ghobrial, Ali, and Hussien, 1978].

On the other hand, large nuclear explosions can generate very strong updrafts which loft quite large particles to high altitudes. Some estimate of the vertical component can be gained by dividing the fireball stabilization altitude, typically on the order of 10-13 km, by the time to rise to that altitude of  $\sim 10$  minutes. Thus, average vertical velocities of 20 m/sec are likely in nuclear explosions. Consequently, particles of radii much greater than  $3 \times 10^{-3}$  m would probably not be lofted to the fireball-stabilization altitude. It should be noted that the density and viscosity of air at the

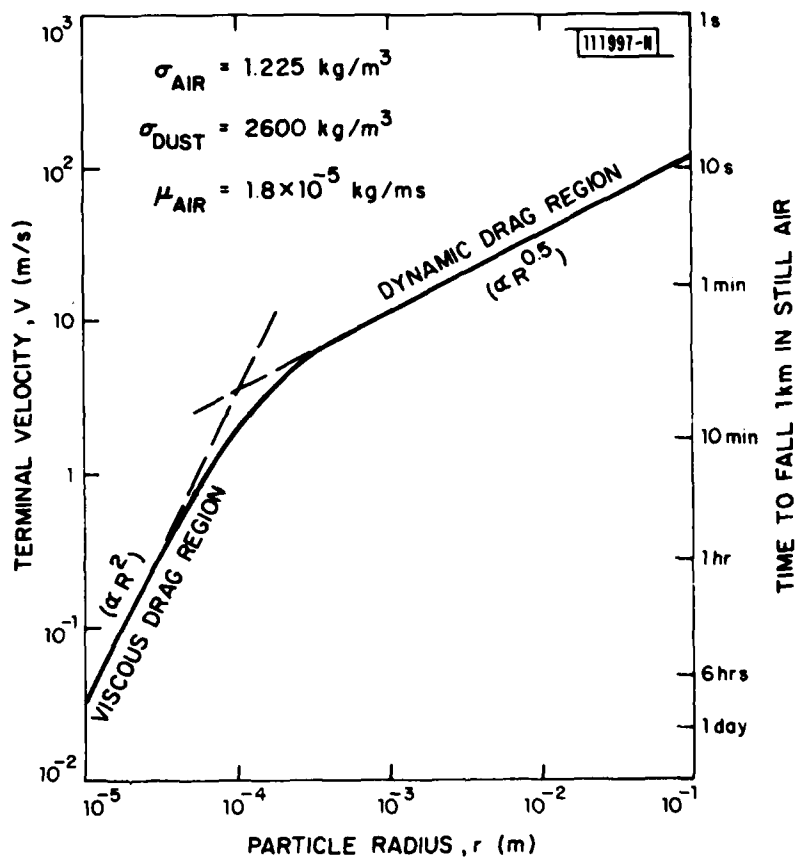


Fig. 2.4.1.1. Terminal velocities of small spherical particles falling in still air at sea level.

higher altitudes is less and the lofting of a given size particle requires a higher vertical velocity than at sea level; therefore, the larger particles will not stay at altitude for long and most of the dust cloud will be composed of particles with radii less than  $10^{-3}$  m\*.

#### 2.4.2 Sandstorms and Dust Storms

Sandstorms and dust storms are two quite different phenomena. What are often called sandstorms, because they occur in arid regions, are really dust storms. Where the surface is alluvial, and not sandy, such as in Iraq or the Sudan around Khartoum, storms called "haboobs" will produce vast dust clouds rising more than 1000 meters into the air and obscuring the sun for long periods [Bagnold, 1941; Lawson, 1971, Idso, Ingram and Pritchard, 1972]. True sandstorms, on the other hand, seldom rise above 2 meters and often, except at the beginning of the storm, the air will be clear and the sun shining on the heads of those who are walking around in what appears to be a "sea of sand" [Bagnold, 1941].

The movement of the sand in a true sandstorm is primarily by saltation [Bagnold, 1941], a mechanism in which the sand grains are propelled forward by the wind and, upon impacting the rough surface material at a shallow angle, rebound upwards to be driven further down wind. One would expect a very pronounced density gradient with altitude in a sandstorm. Effects upon propagation should be limited to terrestrial paths and, in addition, only those paths at extraordinary low heights above the earth would be expected to show substantial effects.

Measurements by Chepil [1957] confirm the expected altitude density gradient for the larger particles. During dust storms in Kansas and Colorado in the 1954-55 time frame, roughly an order of magnitude drop in percent composition of particles with diameters ranging from  $2.5 \times 10^{-4}$  to  $10^{-4}$  meters was observed in increasing the sampling height from 2 to 20 feet. At the same

---

\*The "internal velocities associated with torus rotation and turbulence can be significantly higher; however, few of the large particles will "survive" to the stabilization altitude.

time, smaller particles showed virtually no change in representation with sampling altitude. In fact, the smallest particles, with diameters less than  $2 \times 10^{-6}$  meters actually increased with increased sampling altitude. Chepil [1957] also confirmed the "power-law" behavior of particle size distributions originally observed by Bagnold [1941].

Recent measurements on particle-size distributions during Libyan Sahara sandstorms have been made by Schutz and Jaenicke [1974]. Their measurements for light-wind, moderate-wind and sandstorm conditions are shown in Fig. 2.4.2.1. Because other evidence [Cadle, 1966; McCartney, 1976; Junge, 1957] indicates that the value of  $dN/d\log_{10}r$  continues to increase for aerosols down to nearly  $10^{-7}$  meter radius with very nearly the same exponent as it had at  $10^{-6}$  meter, the measured distribution of Schutz and Jaenicke [1974] have been extrapolated as shown. By carrying out the manipulations described earlier in this section, the probability density distributions for the particle radii can be determined. The three probability densities are given in Fig. 2.4.2.2.

Although Bagnold [1941] states that sand and dust particles of all sizes become airborne at any wind velocity, it is easy to see from Fig. 2.4.2.2 that this statement is not strictly correct. The maximum particle size observed in the aerosol increased by a factor of about 4 from very light wind conditions to sandstorm conditions. Moreover, the proportion of larger particles in the aerosol increased with increasing wind, much as one would expect.

With the suspended mass,  $W$ , defined by (2.2.5) as

$$W = N_T \frac{4}{3} \pi r^3 \sigma \quad \text{kg/m}^3 \quad (2.4.1.12)$$

and  $\sigma = 2600 \text{ kg/m}^3$  (see Section 2.5), and with the meteorological range defined by (2.2.9), the various moments and resultant parameters of the dust aerosol can be obtained from Fig. 2.4.1.2. The results are given in Table 2.4.1.1. Note that, although the mean radius does not change much with wind conditions, the higher moments do exhibit pronounced changes. As a result, the equivalent radius,  $r_e$ , and the suspended mass,  $W$ , both increase with increasing wind. They are mathematically coupled in the following relation:

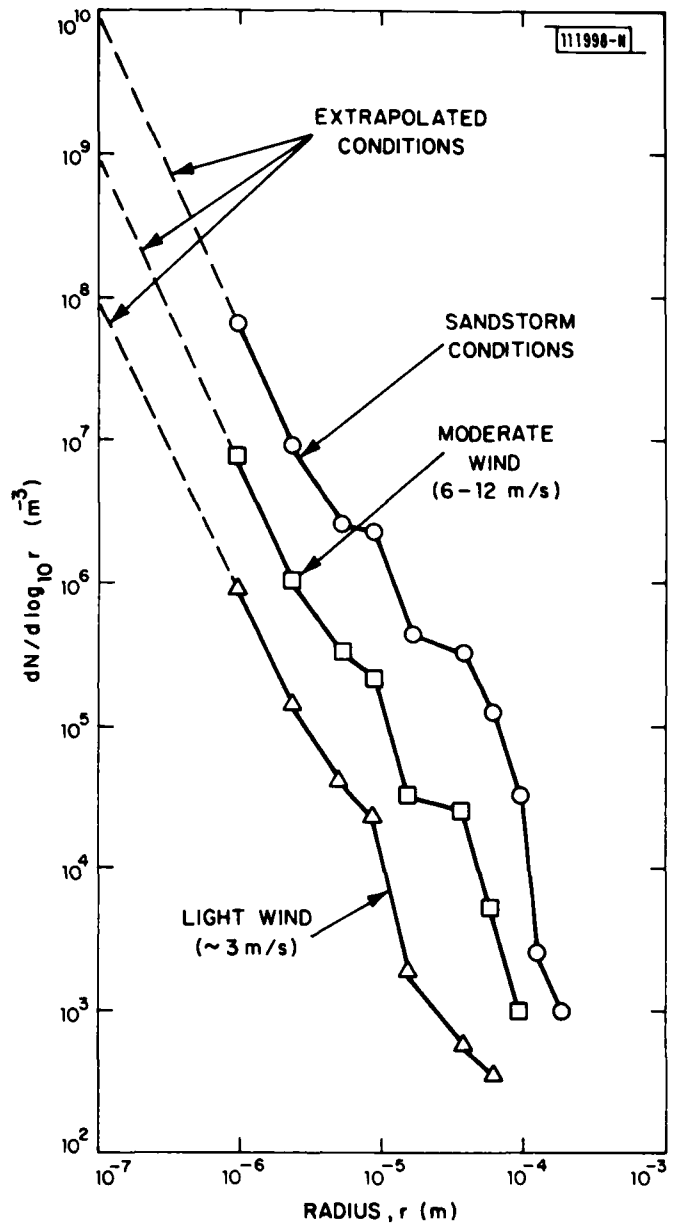


Fig. 2.4.2.1. Measured and extrapolated particle-size distributions for light-wind, medium-wind and sandstorm conditions at Camp Derj in the Libyan Sahara.

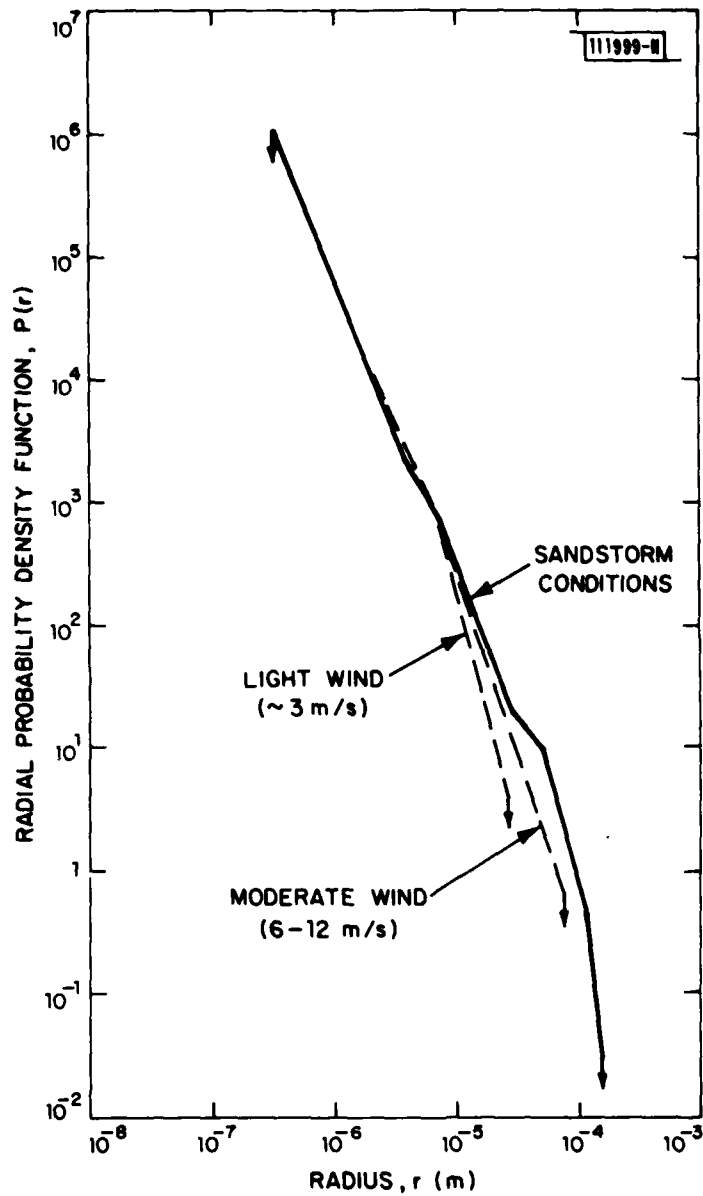


Fig. 2.4.2.2. Probability density distributions for particle radii as determined from the data in Fig. 2.4.2.1.

$$r_e = 8.9 \times 10^{-4} \left( \frac{W}{\sigma} \right)^{0.19} \quad \text{m} \quad (2.4.1.13)$$

so the meteorological range can be written, using (2.2.9), as

$$R_m = \frac{2.3 \times 10^{-3}}{(W/\sigma)^{0.81}} \quad \text{m} \quad (2.4.1.14)$$

It is interesting to note that the Schütz and Jaenicke [1949] data imply substantially greater values of suspended mass than measured by Lawson [1971] during haboobs in Khartoum. Lawson [1971] also quotes Russian measurements on dust storms in the Mangyshalk Peninsula as confirming his observed upper limit for  $W$  of  $4 \times 10^{-5} \text{ kg/m}^3$ . It seems likely that the Libyan measurements of suspended mass by Schütz and Jaenicke [1974] were taken at relatively low elevations [1 to 2 meters] whereas Lawson's were made at an altitude of 10 meters. The Russian sample altitude was 3 meters [Lawson, 1971]. If Chepil's [1957] measurements are correct, however, it is not likely that particles above  $5 \times 10^{-5}$  meters in radius constituted a significant proportion of the sample taken by Lawson. For radio propagation purposes, therefore, the suspended mass densities given in Table 2.4.1.1 should be considered upper bounds.

The meteorological morphology of sandstorms has been discussed in detail by Lawson [1971] and by Idso, Ingram and Pritchard [1972]. Visibility estimates vary widely from the 100-meter values quoted by Al-Hafid, Gupta and Buni [1979] for a "severe" dust storm in Iraq, to a minimum "visibility" of 100 meters by Lawson [1971] in a Sudan haboob, to 400 meters by Idso, Ingram and Pritchard [1972] in an Arizona "haboob". It appears that quoted visibilities in the literature are quite subjective and depend strongly on the incident light intensity. Since sandstorms are often the result of downdrafts from thunderstorms, the reduction in solar flux from the existing clouds may bias the visibility estimates during the dust storm which precedes the thunderstorm. (In fact, many haboobs terminate in a thunderstorm.)



TABLE 2.4.1.1  
SAND- AND DUST-STORM PARAMETERS AS A FUNCTION OF WIND STATE

WIND CONDITIONS	$N_T$ ( $m^{-3}$ )	$\bar{r}$ (m)	$\bar{r}^2$ ( $m^2$ )	$\bar{r}^3$ ( $m^3$ )	$r_e$ (m)	$W$ ( $kg/m^3$ )	$R_m$ (km)
LIGHT (~3 m/sec)	$1.04 \times 10^7$	$4.1 \times 10^{-7}$	$6.9 \times 10^{-13}$	$9.9 \times 10^{-18}$	$1.45 \times 10^{-5}$	$1.13 \times 10^{-6}$	87.2
MODERATE (6-12 m/sec)	$9.4 \times 10^7$	$4.2 \times 10^{-7}$	$1.2 \times 10^{-12}$	$3.6 \times 10^{-17}$	$3.0 \times 10^{-5}$	$3.64 \times 10^{-5}$	5.5
SANDSTORM (up to 50 m/sec)	$8.3 \times 10^8$	$4.4 \times 10^{-7}$	$2.2 \times 10^{-12}$	$1.0 \times 10^{-16}$	$4.7 \times 10^{-5}$	$9.13 \times 10^{-4}$	0.35

The specific meteorological conditions surrounding a "sandstorm" are discussed in detail in Section 2.7. As a final comment here, there does exist data on the probability of occurrence of dust storms [Hoidale, Hinds, and Gomez, 1977]. An example of the diurnal and yearly probabilities of occurrence of blowing dust (defined as visibilities less than 11 km) and dust storms (visibility less than 1 km) are given in Figs. 2.4.2.3 and 2.4.2.4. In addition, in much the same fashion as rainfall [Rafuse, 1980], the duration of the dust storms seems to be lognormally distributed; an example corresponding to the Kuwait data in Figs. 2.4.2.3 and 2.4.2.4. is given in Fig. 2.4.2.5. It seems quite apparent from the data that the probabilities of occurrence are strongly linked to the expected convective weather patterns which peak (in the Northern Hemisphere) in the summer and in the afternoons.

#### 2.4.3 Conventional and Nuclear Explosions

##### 2.4.3.1 Nuclear Explosions

Dust and suspended particulate matter are produced by several different mechanisms in a nuclear detonation. If the detonation height is low enough, a crater is formed and ejecta are produced. As the fireball expands, portions of the crater ejecta are entrained and vaporized. The bomb casing and other nearby materials also contribute to the suspended debris. The thermal pulse from the fireball "popcorns" the first few millimeters of soil into the air as the absorbed water and water of hydration are vaporized. This popcorned dust is raised further by the shock wave from the detonation. As the fireball expands and rises, a stem is formed and the intruding winds scour material from the surrounding ground and crater and introduce it into the stem. If the stem and fireball region are connected, the stem material contributes to the condensed particulate matter in the fireball, as the fireball cools and rises to its stabilization altitude.

From Glasstone [1962] and Thompson [1978] the general characteristics of pedestal, stem and fireball-created cloud can be described in terms of the normalized burst altitude

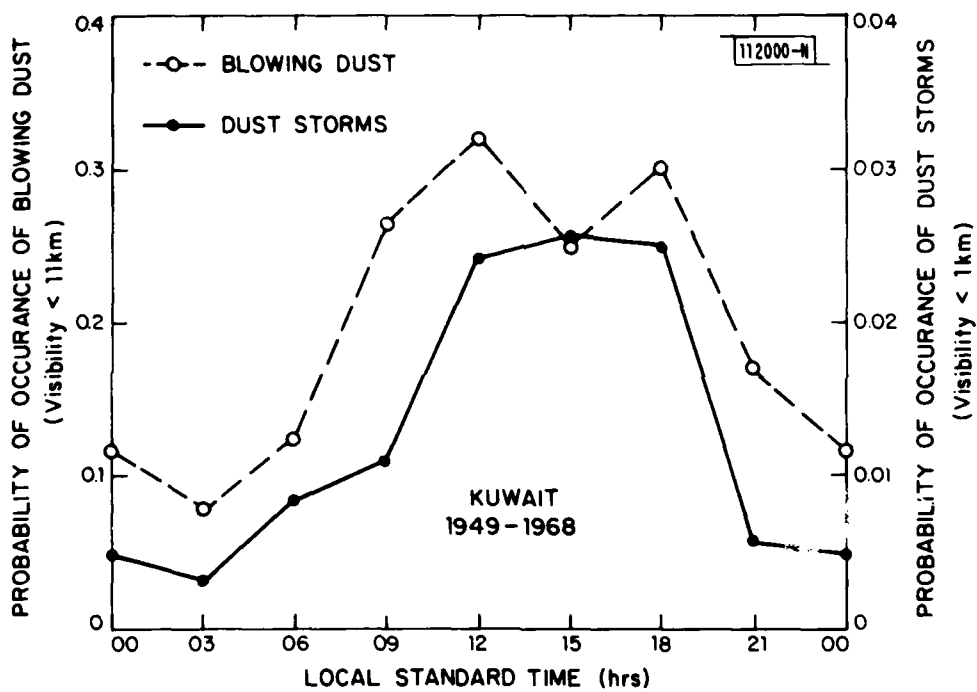


Fig. 2.4.2.3. Diurnal probability of occurrence of blowing dust and dust storms in Kuwait.

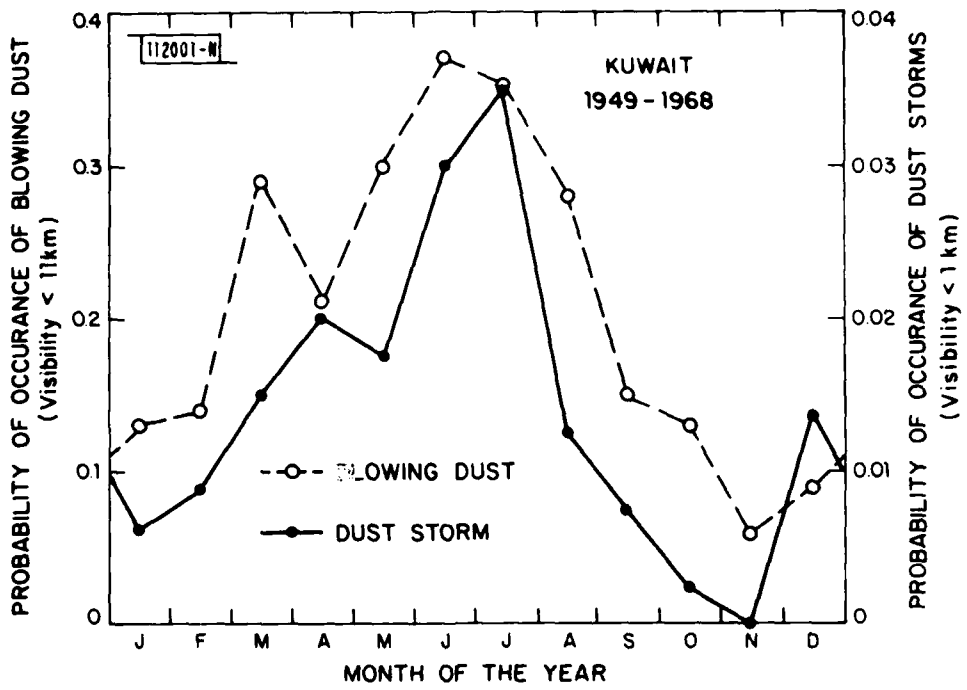


Fig. 2.4.2.4. Yearly probability of occurrence of blowing dust and dust storms in Kuwait.

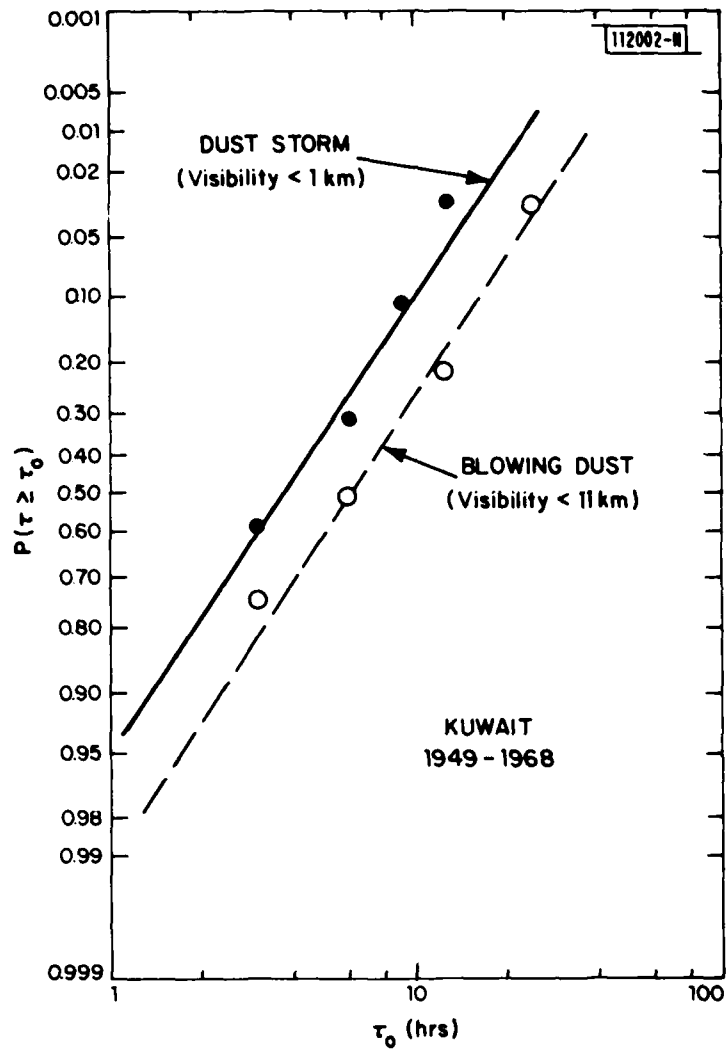


Fig. 2.4.2.5. Cumulative probability density distribution function for the duration of blowing-dust occurrences and dust storms.

$$H_{BO} = H_B / Y^{1/3} \quad \text{m} \quad (2.4.3.1)$$

where  $H_B$  is the burst altitude and  $Y$  is the weapon yield in  $\text{Mt}^*$ . The fireball equilibrium radius will be

$$R_{EQ} = 804 Y^{1/3} \quad \text{m} \quad (2.4.3.2)$$

Using these definitions, the dust characteristics are identified in Table 2.4.3.1. Once stabilized at maximum altitude, the so-called "10-minute" cloud radius is [Cadle, 1966]

$$R_{10} = 16,000 Y^{1/3} \quad \text{m} \quad (2.4.3.3)$$

Of course, the high altitude cloud behavior is strongly influenced by the upper-altitude winds.

Various models for the dust entrainment behavior have been generated. From Thompson [1978], a model for the final yield-normalized radius and height of the pedestal is given in Fig. 2.4.3.1. The resulting yield-normalized density of suspended particulate matter is given in Fig. 2.4.3.2. A model for the yield-normalized stem radius is

$$R_s / Y^{1/3} = \begin{cases} 488, & 0 < t/Y^{1/3} < 60 \\ 63 \left( \frac{t}{Y^{1/3}} \right)^{1/2}, & 60 < t/Y^{1/3} < 1000 \\ 2000, & 1000 < t/Y^{1/3} \end{cases} \quad \text{m}/(\text{Mt})^{1/3} \quad (2.4.3.4)$$

with a stem dust density described as

$$W_s(t) = \text{Max} \left\{ 2.5 \times 10^{-2} e^{-t/6.34}, \hat{W}_s \left( \frac{R_I}{R_s(t)} \right)^2 \right\} \quad \text{kg/m}^2 \quad (2.4.3.5)$$

\* Megatons (of TNT).

TABLE 2.4.3.1  
 DUST FORMATION CHARACTERISTICS OF A NUCLEAR DETONATION  
 AS A FUNCTION OF NORMALIZED BURST ALTITUDE

<u>H<sub>90</sub> (m)</u>	<u>CHARACTERISTICS</u>
0-240	Crater formation with ejecta; Stem, pedestal and fireball connected; Substantial mixing.
240-2060	Compaction crater only; No ejecta; Pedestal composed of popcorned materials; Pedestal, stem and fireball connected; Substantial mixing.
2060-2400	No crater; No pedestal formation; Stem composed of popcorned material; Stem connected to fireball with mixing.
2400-4800	No crater; No pedestal; Stem disconnected from fireball; No mixing.
>4800	No dust.

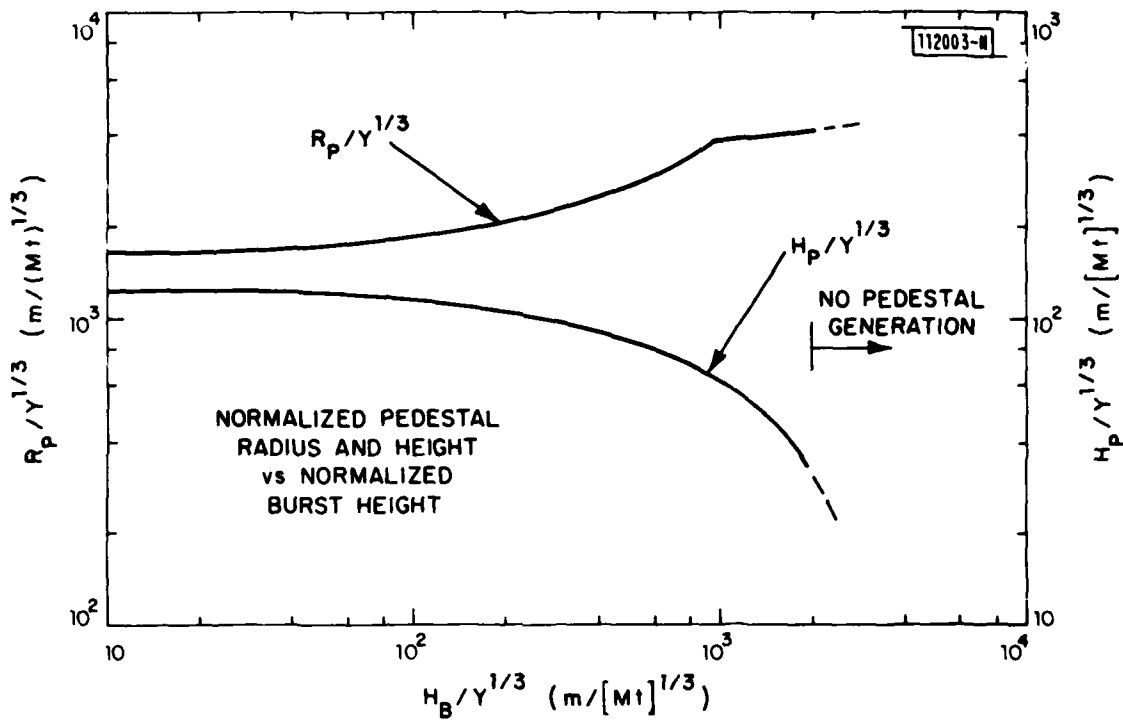


Fig. 2.4.3.1. Normalized pedestal radius and height versus normalized burst height.



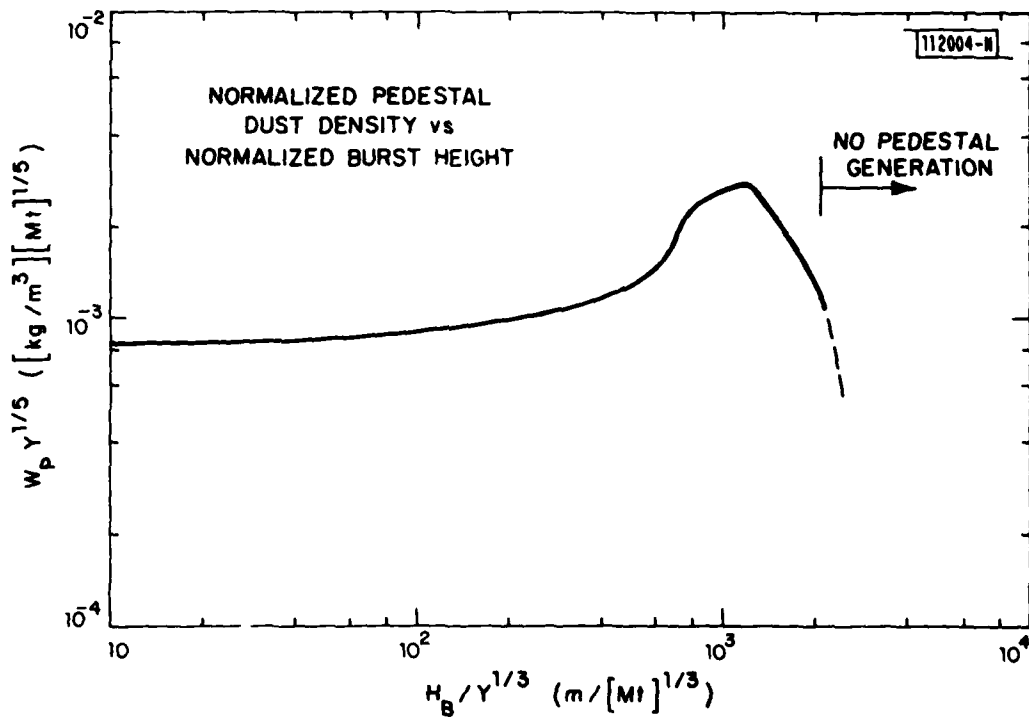


Fig. 2.4.3.2. Normalized pedestal dust density versus normalized burst height.

with  $t$  in seconds and

$$\hat{W}_s = \begin{cases} 5.2 \times 10^{-4} Y^{1/3}, & 0 < Y < 5 \\ 8.9 \times 10^{-4}, & Y > 5 \end{cases} \quad \text{kg/m}^3 \quad (2.4.3.6)$$

and

$$R_I = 732 Y^{1/3} \quad \text{m} \quad (2.4.3.7)$$

As an example, consider the dust generated by a 100-kt detonation at a height of 100 meters. The normalized burst height is 215 meters so a crater with some ejecta is formed and the pedestal, stem, and fireball are all connected with substantial mixing. The equilibrium radius for the fireball will be 373 meters and the 10-minute cloud radius will be 7.4 km at an altitude of 13 km [Glasstone, 1962] and with probable thickness of about 1 km.

The pedestal will be about 1900 meters in diameter and 97 meters high with a suspended dust density of  $4.6 \times 10^{-4} \text{ kg/m}^3$ . The stem radius behavior with time will be

$$R_s = \begin{cases} 227, & 0 < t < 28 \\ 42.9t^{1/2}, & 28 < t < 464 \\ 928, & 464 < t \end{cases} \quad \text{m} \quad (2.4.3.8)$$

with a suspended dust density versus time given in Fig. 2.4.3.3. Fireball dust densities must be equal to or lower than those of the stem because the stem is the major source of particulate matter for the fireball. As the fireball expands, rises, and reaches its stabilization altitude, the density of suspended dust will drop. However, because of geometric factors, the path-

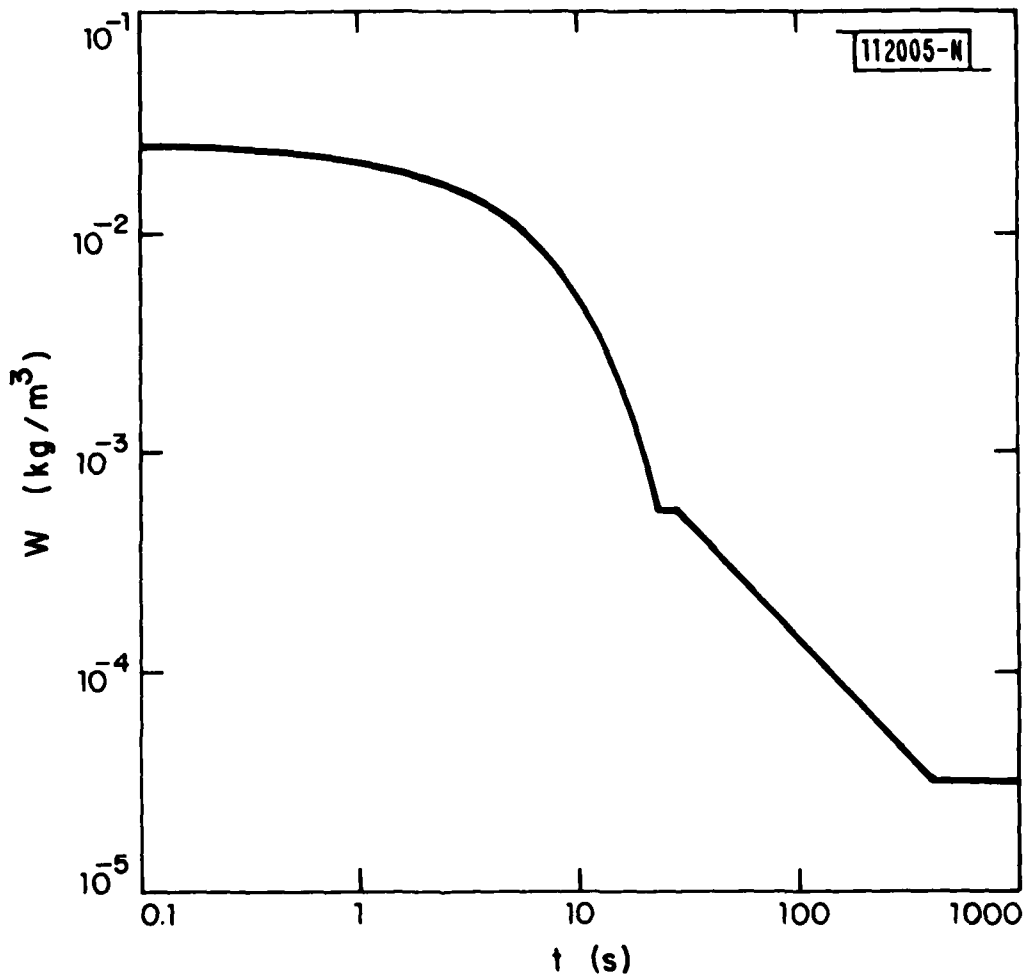


Fig. 2.4.3.3. Stem-region suspended mass density as a function of time for a 100-kt detonation at 100-meter altitude.

integrated dust density would be expected to show a slower drop with time, unless fallout is able to keep up with the geometric factors.

If dust densities in a nuclear or conventional explosion become too high, the particles no longer behave as individuals. In this case, the particles entrap the air and fall as a single mass and the individual particle terminal velocities cited in Section 2.4.2 no longer hold. This mechanism is responsible for a phenomenon known as "base surge" [see Cadle, 1966] and was particularly evident in the Bikini underwater bursts and the Jangle underground shot in Nevada.

Thompson [1978] suggests a probability density distribution for the suspended particle radius which is a hybrid between lognormal for small radii and power-law for large radii. As a result of an examination of the optical and radio properties of his dust model and with knowledge of the ability of the natural aerosol-size power law to extend to submicron sizes, the use of the power-law model alone becomes quite attractive. There will, of course, be some condensation and agglomeration taking place as the fireball cools, plus some nucleation rain formed if atmospheric parameters are favorable. Both of these effects will tend to reduce the particle number density with radii less than 1  $\mu\text{m}$ . However, for the purposes of this study a simple -3.5 power law probability density function will be chosen as representative of the behavior of cohesive soil [Thompson, 1978].

Since the fall time from a 1-km altitude of a 0.05-m radius particle is less than 10 seconds [see Fig. 2.4.1.1], Thompson's [1978] upper limit for particle diameter of 0.1 meter will be assumed to hold only for the early time period in the explosion (i.e., the first 10 to 30 seconds or so). After that initial period, much of the larger debris has fallen out and the particle sizes will be assumed to truncate at a radius of  $3 \times 10^{-3}$  meters. This "late-time" truncation radius value is indicated by a rough bound on the vertical velocities in the stem region of about 20 m/sec (set by an assumed stabilization altitude of 13 km reached in about 10 minutes).

Under these assumptions, the probability density function for the radius of the suspended particles in a nuclear (or conventional) explosion will be\*

$$p(r) = 2.5 \times 10^{-15} r^{-3.5} \text{ m}^{-1} \quad (2.4.3.9)$$

for

$$\text{EARLY TIME} \quad 10^{-6} < r < 10^{-1} \text{ m}$$

$$\text{LATE TIME} \quad 10^{-6} < R < 3 \times 10^{-3} \text{ m}$$

The pdf in (2.4.3.9) will have virtually the same mean and mean-square radii in either early or late time periods. Only the values of  $\overline{r^3}$  will be much different. (Note that the rapid fallout of larger particles from the stem region is mirrored in the first term in (2.4.3.5).)

The radial moments and suspended mass densities for the stem and pedestal regions of a 100-kt, 100-meter-altitude detonation are shown in Table 2.4.3.2. The models are very crude and do not include such effects as smoke generated by detonation-induced fires and water-vapor condensation in the nuclei-rich cloud.

If the smallest particle size stays at  $10^{-6}$  meter (radius) and the exponent changes to -4.5 to represent fine sandy/silty soil [Thompson, 1978], then the pdf is changed significantly. The moments for late- and early-time behavior are essentially equal and the value of  $r_e$  drops to  $3 \times 10^{-6}$  m for each case. This is to be expected for the fine, dusty soil characteristics of, for example, the central US.

---

\*Note that the contribution from particles with radii lying between  $3 \times 10^{-3}$  and  $10^{-1}$  meters is so small that the form of  $p(r)$  in (2.4.3.4) does not change significantly with time.

TABLE 2.4.3.2  
STEM AND PEDESTAL DUST PARAMETERS FOR A 100-kt DETONATION OVER COHESIVE SOIL  
AT AN ALTITUDE OF 100 METERS

EPOCH	<u>100-kt Explosion Stem Parameters</u>				
	$\bar{r}$ (m)	$\bar{r}^2$ (m <sup>2</sup> )	$\bar{r}^3$ (m <sup>3</sup> )	$r_e$ (m)	$W$ (kg/m <sup>3</sup> )
EARLY (T<6 SEC)	$1.67 \times 10^{-6}$	$4.98 \times 10^{-12}$	$1.85 \times 10^{-15}$	$3.2 \times 10^{-4}$	$2.5 \times 10^{-2}$
MEDIUM (T~60 SEC)	$1.67 \times 10^{-6}$	$4.95 \times 10^{-12}$	$6.57 \times 10^{-16}$	$1.3 \times 10^{-4}$	$2.5 \times 10^{-4}$
LATE (T>360 SEC)	$1.67 \times 10^{-6}$	$4.91 \times 10^{-12}$	$2.69 \times 10^{-16}$	$5.5 \times 10^{-5}$	$3.2 \times 10^{-5}$
	<u>100-kt Explosion Pedestal Parameters</u>				
EARLY TO MEDIUM	$1.67 \times 10^{-6}$	$4.95 \times 10^{-12}$	$6.57 \times 10^{-16}$	$1.3 \times 10^{-4}$	$4.64 \times 10^{-4}$

#### 2.4.3.2 Conventional Explosions

Conventional explosions also raise clouds of dust. However, the thermal effects are much reduced, over the nuclear counterpart, and most of the particulate matter is generated by the shock wave and the inrush of air as the hot gases rise to produce a mini "mushroom cloud". Surface bursts of large charges of conventional explosives produce dust clouds not unlike those of a nuclear explosion [Burns and Crawley, 1979; Burns, 1977]. However, because there is no true fireball, the thermal effects are reduced and the "scouring" effect of inrush winds is less.

On a much smaller scale, the explosion of a conventional weapon produces a smoke cloud composed of particulate matter from the combustion products. The smoke cloud, because of the small effective radius of the particles, will be optically quite dense even though the suspended mass fraction,  $W/\sigma$ , might be rather small. The rf effects should be negligible.

#### 2.4.4 Comparisons

A comparison of the radial pdf's for sandstorms (in reality, dust storms) and nuclear detonations over cohesive soil or rock (-3.5 exponent) and fine sandy/silty soil (-4.5 exponent) are shown in Fig. 2.4.4.1\*. Of more interest is the suspended matter density and equivalent radii for the various processes. Using a density of  $2600 \text{ kg/m}^3$  for the particle material, the four nuclear-detonation states are compared with the sandstorm from Section 2.4.2 in Table 2.4.4.1.

As one would expect, the late-time behavior of a nuclear burst over dusty, fine soil is sensibly the same as that of a dust storm. Over cohesive or rocky soil much less particulate matter is swept up in the fireball. One should note that the rf path length through a dust storm would extend for several kilometers (2 to 10) whereas, in the stem region at least, the rf path

---

\*An exponent of -4 would be expected for the fine, alluvial soils characteristic of desert regions.

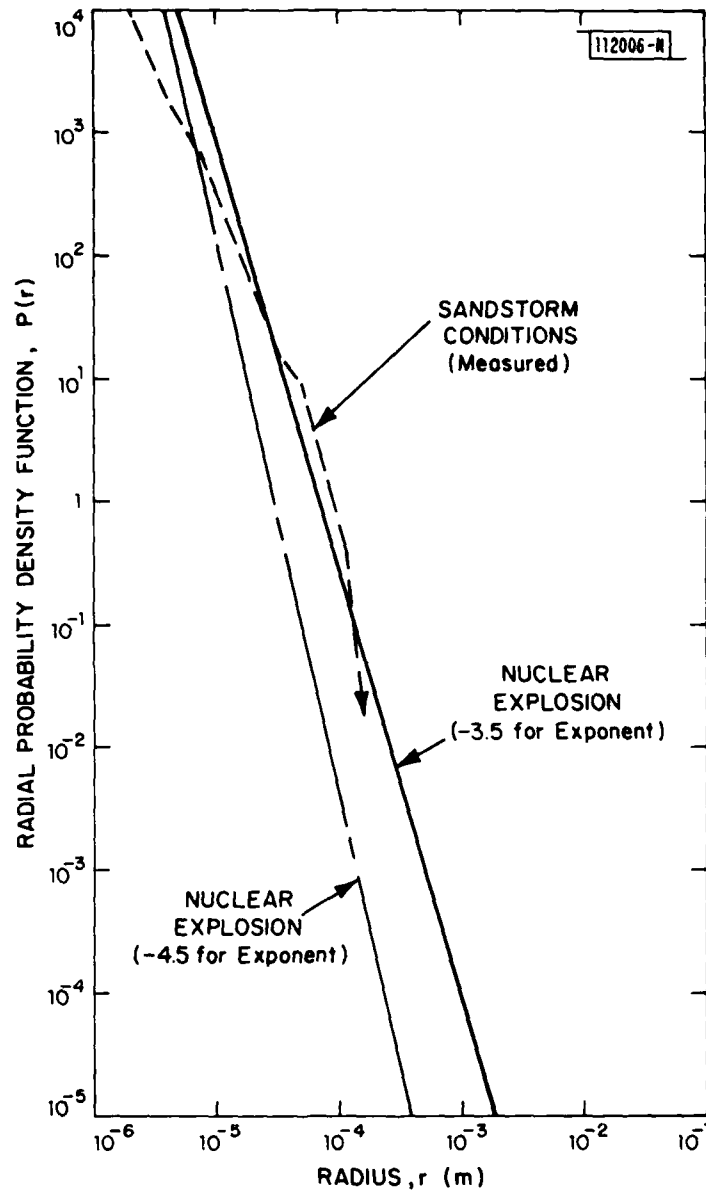


Fig. 2.4.4.1. Radial probability density distributions for nuclear detonations over two soil extremes and a sandstorm.



TABLE 2.4.4.1  
 COMPARISON OF EFFECTIVE RADIUS,  $r_e$ , SUSPENDED MASS,  $W$ , AND METEOROLOGICAL RANGE,  $R_m$ ,  
 FOR NUCLEAR DETONATIONS OVER TWO SOIL EXTREMES AND A SANDSTORM

<u>PROCESS</u>	<u><math>r_e</math> (m)</u>	<u><math>W</math> (kg/m<sup>3</sup>)</u>	<u><math>R_m</math> (km)</u>
NUCLEAR EARLY COHESIVE SOIL	$3.2 \times 10^{-4}$	$2.5 \times 10^{-2}$	0.087
NUCLEAR LATE COHESIVE SOIL	$5.5 \times 10^{-5}$	$3.2 \times 10^{-5}$	11.7
NUCLEAR EARLY FINE SANDY SOIL	$3 \times 10^{-6}$	$2.5 \times 10^{-2}$	0.001
NUCLEAR LATE FINE SANDY SOIL	$3 \times 10^{-6}$	$3.2 \times 10^{-5}$	0.64
SANDSTORM	$4.7 \times 10^{-5}$	$9.1 \times 10^{-4}$	0.35

through the nuclear-generated dust will be much less. A better comparison might be the product of path length and suspended mass,  $WD$ , in  $\text{kg}/\text{m}^2$ .

For example, in the stem region of the 100-kt example in Section 2.4.3 the stem diameter (see (2.4.3.8)) increases from 454 to 1860 meters as time progresses. The maximum integrated density still occurs for  $t$  small and amounts to  $11.4 \text{ kg}/\text{m}^2$ , then the integrated density drops rapidly to a final value of  $5.95 \times 10^{-2} \text{ kg}/\text{m}^2$ . A 10-kilometer path through a typical sandstorm would have an integrated density of  $9.1 \text{ kg}/\text{m}^2$ . Consequently, due to the suspended dust, the initial rf performance of a path through the stem of a nuclear detonation dust cloud would be virtually the same as through a sandstorm and, as time progressed, the effects of the stem dust would become much less than those in a sandstorm. In similar fashion, the total integrated dust in a path through the fireball should drop as the fireball expands, because the entrained mass of dust is essentially constant and its density must drop as the cube of the cloud radius.

It should be noted that the rf effects of a dust cloud are proportional directly to the fractional mass lofted,  $W/\sigma$  (see Section 2.3). The optical effects, however, are proportional to the product of mass fraction and the reciprocal of the equivalent radius,  $r_e$  (see Section 2.2). Consequently, the same mass fraction with the same rf attenuation and phase shift can have very different optical properties. Very fine soil with  $r_e \sim 3 \times 10^{-6}$  meters will produce an order-of-magnitude greater optical attenuation for the same mass of dust as that produced by alluvial desert-region soils and two orders-of-magnitude greater optical attenuation than dust produced by explosions over rock and/or highly cohesive soils.

## 2.5 Material Constants

Typical values for the density,  $\sigma$ , are  $2600 \text{ kg}/\text{m}^3$  for terrestrial materials such as sand. Since sand is mostly silicon dioxide (quartz) this figure compares favorably with the quoted density for quartz of  $2650 \text{ kg}/\text{m}^3$ . On the other hand, clays contain significant amounts of alumina with a density

of  $3800 \text{ kg/m}^3$  but also contain more water, both of hydration and trapped in interstices, so the density of clay grains will be less than that of pure alumina, but much greater than the  $1000 \text{ kg/m}^3$  for water. For the purposes of this section\* clay particles will be assumed to have the same density as sand,  $\sigma=2600 \text{ kg/m}^3$ . Note that the volume fraction,  $W/\sigma$ , for dry soil, either loose or compacted, is significantly less than unity and the density and dielectric constant of bulk soil would not be the correct value to use for the density and dielectric constant of the individual particles which make up the soil.

The relative dielectric constant of sand particles was assumed by Chu [1979] to be the same as the bulk value for soil quoted in the Reference Data for Radio Engineers [1968]. The value chosen of 2.5 [1-j0.01] is not representative of quartz. From the same handbook the relative dielectric constant of fused quartz is  $3.78[1-j2.5 \times 10^{-4}]$  at 25 GHz. However, the water trapped in the terrestrial sand particles will raise the microwave loss tangent substantially.

A measurement of the real part of the refractive index and the loss tangent of the refractive index of air suspensions of sand and clay grains was made by Ahmed and Auchterlonie [1976]\*\*. From their measurements at 10 GHz with values of  $\text{Re}\{n\}$  and  $\text{Im}\{n\}$  given as functions of  $W$  and by assuming a value of  $\sigma=2600 \text{ kg/m}^3$ , the following relative dielectric constants for sand and clay can be found using (2.3.5):

---

\*For most purposes,  $\sigma=2600 \text{ kg/m}^3$  is an adequate value for almost all suspended soil particles. Vegetative particles might well be lighter. For this report the density of all dust particles will be assumed to be that given here.

\*\*Additional measurements on sand and caliche (calcium carbonate) samples were made by Burns and Winkelman and reported by Burns and Crawley [1979]. Their sand results gave somewhat larger values of  $\epsilon'$  and  $\tan\delta$  than those quoted here, perhaps because of a higher moisture content in the Burns and Winkelman samples. Their caliche results were somewhat less than those quoted here for clay.

$$\epsilon' = 3.36 \pm 0.19$$

SAND

$$\tan\delta = 0.025 \pm 0.011$$

$$\epsilon' = 7.09 \pm 0.88$$

CLAY

$$\tan\delta = 0.29 \pm 0.05$$

Generally, the loss tangents and dielectric constants are almost constant above 3 GHz, so these 10-GHz values could be expected to be valid to 44 GHz and beyond.

The real part of the dielectric constant for fused quartz is 3.78 and that for alumina is 8.8. The measured values of Ahmed and Auchterlonie [1976] are in good agreement with the values for the pure ingredients. The sand grains have a much larger loss tangent than fused quartz because of water with some dissolved solids trapped in the surface and volume cracks in the grains. Similarly, the clay particles measured would be expected to have substantial water content, both of hydration and trapped in interstices, and this water would be expected to reduce the density of the clay grains below that of alumina ( $3800 \text{ kg/m}^3$ ), reduce the relative dielectric constant (8.8 for alumina), and greatly increase the loss tangent. All three effects are, in fact, observed (as well as the expected slight reduction in  $\epsilon'$  for sand relative to fused quartz).

#### 2.6 Comparison of Fog and Dust

Because fogs are probably at least as prevalent as dust storms (although not usually in the same geographical location) and because nucleation clouds are a common occurrence in large nuclear-weapon detonations, it is of interest to compare optical and millimeter-wave attenuations and phase shifts due to dusts and fogs. For a fog, as for dust, the meteorological range is given by (2.2.9) as

$$R_m = 2.608 r_e \left( \frac{\sigma}{W} \right) \quad m \quad (2.6.1)$$

In much of the literature the term  $W/\sigma$ , which represents the suspended mass fraction, is often written as  $\ell w$ , the liquid water content [McCartney, 1976]. Properly speaking, however, measured  $\ell w$  is given the dimensions of  $\text{gm/cm}^3$  or  $\text{kg/m}^3$  and great care must be taken to normalize with respect to the proper density,  $1 \text{ gm/cm}^3$  or  $1000 \text{ kg/m}^3$  depending on the units (for  $\ell w$  in  $\text{gm/m}^3$ , a multiplication of  $10^6$  is necessary to achieve a correct value of  $W/\sigma$ ).

The rf behavior is determined by the complex dielectric constant of water. Table 2.6.1, taken from Koester and Kosavsky [1971], gives the temperature dependence for the constants inserted in the Debye formula for relative dielectric constant

$$\epsilon = \frac{\epsilon(0) - \epsilon(\infty)}{1 + j \frac{\Delta\lambda}{\lambda}} + \epsilon(\infty) \quad (2.6.2)$$

For this example, a temperature of  $10^\circ\text{C}$  is chosen, so the relative dielectric constant for the fog droplets can be written as

$$\epsilon = \frac{78.5}{1 + j 7.47 \times 10^{-2} f_{\text{GHz}}} + 5.5 \quad (2.6.3)$$

where  $f_{\text{GHz}}$  is the operating frequency in GHz. In this case,

$$\frac{\epsilon - 1}{\epsilon + 2} = \frac{7138 + 0.188 f_{\text{GHz}}^2}{7396 + 0.3136 f_{\text{GHz}}^2} - j \frac{17.584 f_{\text{GHz}}}{7396 + 0.3136 f_{\text{GHz}}^2} \quad (2.6.4)$$

Assuming Rayleigh scattering, the excess phase shift and loss can be obtained by inserting (2.6.4) in (2.3.8) and (2.3.9). The results are

$$\Delta\theta = \frac{1.737 \times 10^6 f_{\text{GHz}} + 45.75 f_{\text{GHz}}^3}{1 + 4.24 \times 10^{-5} f_{\text{GHz}}^2} \left[ \frac{W}{\sigma} \right] \quad \text{0/km} \quad (2.6.5)$$

and

TABLE 2.6.1  
 TEMPERATURE DEPENDENCE OF THE CONSTANTS IN THE DEBYE FORMULATION OF (2.6.2)

$T(^{\circ}\text{C})$	$\epsilon(0)$	$\epsilon(\infty)$	$\Delta\lambda(\text{cm})$
0	88.0	5.5	3.59
10	84.0	5.5	2.24
18	81.0	5.5	1.16
20	80.0	5.5	1.53
30	76.4	5.5	1.12
40	73.0	5.5	0.857

$$L = \frac{649 f_{\text{GHz}}^2}{1+4.24 \times 10^{-5} f_{\text{GHz}}^2} \left[ \frac{W}{\sigma} \right] \quad \text{dB/km} \quad (2.6.6)$$

In a fog, in much the same manner as in a dust storm (see Section 2.4.2), the meteorological range is given as [McCartney, 1976]

$$R_m = \frac{3.02 \times 10^{-3}}{[W/\sigma]^{0.65}} \quad \text{m} \quad (2.6.7)$$

The reason for the fractional exponent on  $W/\sigma$  for a fog, however, is different from that used to obtain the fractional exponent on  $W/\sigma$  for dust storms. For dust storms an increasing wind sweeps up larger and larger particles, so as  $N_T$  increases so does  $r_e$  (but at a slower rate). For a fog, the number of nuclei remain sensibly constant with time, but the droplet radii increase to increase  $W/\sigma$ ; thus,  $r_e$  is approximately proportional to  $(W/\sigma)^{0.33}$ .

By substituting (2.6.7) into (2.6.5) and (2.6.6), the excess phase and loss can be written as

$$\Delta\theta = \frac{231 f_{\text{GHz}} - 6.1 \times 10^{-3} f_{\text{GHz}}^3}{1+4.24 \times 10^{-5} f_{\text{GHz}}^2} \frac{1}{R_m^{1.54}} \quad \text{°/km} \quad (2.6.8)$$

and

$$L = \frac{8.6 \times 10^{-2} f_{\text{GHz}}^2}{1+4.24 \times 10^{-5} f_{\text{GHz}}^2} \frac{1}{R_m^{1.54}} \quad \text{dB/km} \quad (2.6.9)$$

where  $R_m$  is given in meters.

Using the material constants for sand given in Section 2.5, the dust-storm value for Rayleigh scattering becomes

$$\frac{\epsilon-1}{\epsilon+2} = 0.44 - j8.8 \times 10^{-3} \quad (2.6.10)$$

and, from (2.4.1.14), the meteorological range in a dust storm becomes

$$R_m = \frac{2.3 \times 10^{-3}}{[W/\sigma]^{0.81}} \quad \text{m} \quad (2.6.11)$$

These two values, inserted into (2.3.8) and (2.3.9) give the dust storm excess phase and loss as

$$\Delta\theta = 4.4 \times 10^2 f_{\text{GHz}} \frac{1}{R_m^{1.23}} \quad \text{°/km} \quad (2.6.12)$$

and

$$L = 1.34 f_{\text{GHz}} \frac{1}{R_m^{1.23}} \quad \text{dB/km} \quad (2.6.13)$$

where, as before,  $R_m$  is in meters.

A severe sandstorm might have visibility reduced to 100-200 meters while thick fog would have a visibility reduced to 20-50 meters. The greater effectiveness of fog in reducing visibility comes about in part from the smaller exponent in the size distribution (-2 for  $dN/d\log_{10}r$  versus  $r$ ) and in part from the smaller density giving a larger value of mass fraction for a given suspended mass. It seems reasonable to compare worst-case values. Table 2.6.2 compares the 11-GHz and 44-GHz excess phase shifts and attenuations due to the particulate matter in a worst-case fog and a worst-case sandstorm.

From the tabulation, it can be seen that at 11 GHz the worst-case fog and worst-case dust storm have virtually identical effects. At 44 GHz, the excess phase shifts for the fog and dust are essentially the same, but, as one might expect, the dB loss per km in the fog is almost an order-of-magnitude greater.

## 2.7 The Forgotten Parameter: Changes in Atmospheric Refractive Index Not Connected with Dust Content

If the potential effects of a severe sandstorm (dust storm) at 11 GHz are computed, the measured values of  $W/\sigma$ ,  $r_e$  and  $R_m$  from Section 2.4, coupled with



TABLE 2.6.2  
 COMPARISON OF WORST-CASE FOG AND DUST EXCESS PHASE AND ATTENUATION AT 11 AND 44 GHz

<u>FREQUENCY</u>	FOG ( $R_m=20-50$ m)		SANDSTORM ( $R_m=100-200$ m)	
	$\Delta\theta$ ( $^\circ/\text{km}$ )	<u>L (dB/km)</u>	$\Delta\theta$ ( $^\circ/\text{km}$ )	<u>L (dB/km)</u>
11	6-25	0.025-0.10	7-17	0.02-0.05
44	24-98	0.37-1.5	29-67	0.085-0.20

the measured dielectric constant values from Section 2.5, yield an excess phase shift of  $\sim 3.1^\circ/\text{km}$  and a loss of  $9.3 \times 10^{-3}$  dB/km under nominal sandstorm conditions with  $R_m = 0.35$  km. For a microwave link with terminals elevated 50 m at each end, the useful maximum path would be limited to about 40 km. Consequently, roughly  $120^\circ$  of phase shift and 0.37 dB of attenuation would be expected during a sandstorm.

If the total phase shift amounted to many radians then natural turbulence and the resulting refractive inhomogeneities could be invoked to produce multipath fading. Such, however, is not the case. How, then, can one explain the 2- to 4-dB median signal reduction and 10- to 15-dB fades observed in Iraq on an 11-GHz microwave link during a sandstorm [Al-Hafid, Gupta, and Buni, 1979; Al-Hafid, Gupta, and Ibrahim, 1980]? It does not seem as if the measured suspended-mass densities can produce the effects observed.

The papers by Lawson [1971] and Idso, Ingram and Pritchard [1972] on haboobs provide the clues. Since most dust storms are produced by downdrafts from thunderstorms, even though no rain may reach the ground, rain-cooled air is thrust down from the storm and out along the ground under the warm, dry, pre-existing air mass. The mini-frontal structure moves forward at a velocity approximately one-half the maximum wind speed behind it [Lawson, 1971]. The division between the advancing moist, cool air and the warm air is very marked, with temperature differences of up to  $15^\circ\text{C}$  observed within a distance of less than 50 m [Lawson, 1971]. Very often, because of the manner in which the lobes of the advancing mini-front are generated, mature, and then slow, with new lobes appearing to either side, large warm patches of air are found imbedded in the cool air behind the front [Lawson, 1971]. The dust fills in the lobes, giving them excellent visibility and allowing detailed observations of the time structure to be made with ease.

The vertical structure of the lobes, which agrees well with tank experiments in the laboratory, and with observations on haboobs, is shown in Fig. 2.7.1. Typical maximum heights average between 1000 and 2000 meters. The haboobs in Khartoum have a maximum speed of advance of 70 to 80 kph (19 to

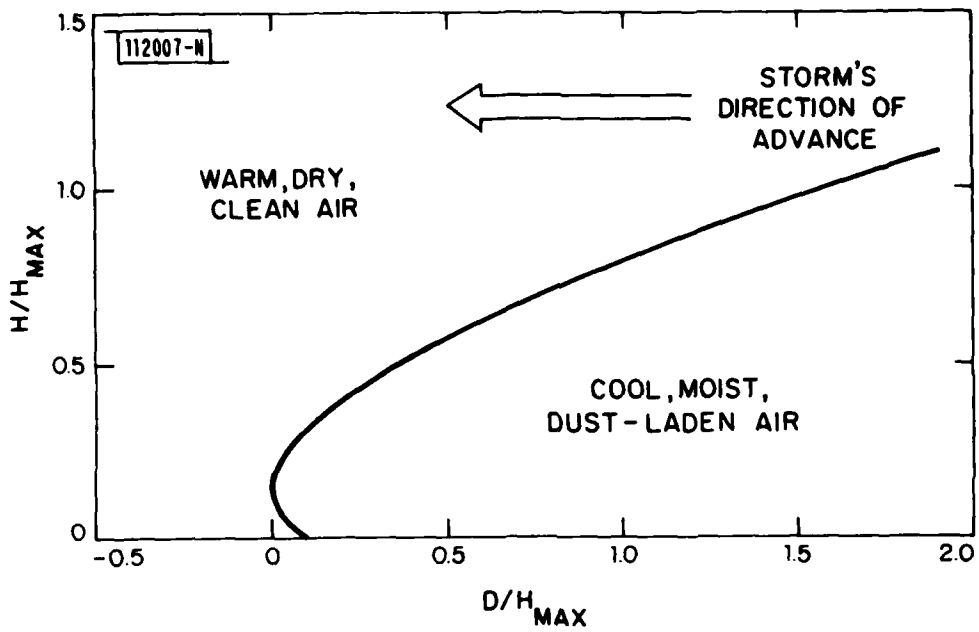


Fig. 2.7.1. Vertical structure of the advancing lobe of a haboob given with the height,  $H$ , and distance into the lobe,  $D$ , normalized with respect to the maximum lobe height,  $H_{max}$  (typically 1000 to 2000 m).

22 m/sec) so maximum wind velocities behind the front can be expected to range up to 140 to 160 kph (39 to 44 m/sec). Similar characteristics have been observed in Arizona haboobs by Idso, Ingram and Pritchard [1972].

As is well known, the refractive index of the atmosphere is a function of the temperature, pressure and water content (humidity). From the Handbook of Geophysics [1961], the excess refractive index at radio frequencies, defined as\*

$$N = (n-1) \times 10^6 \quad (2.7.1)$$

is

$$N = \frac{0.776 P}{T} + \frac{3.7 \times 10^3 P_{WV}}{T^2} \quad (2.7.2)$$

where

P is the pressure in  $N/m^{2**}$ ,

T is the temperature in kelvins, and

$P_{WV}$  is the partial pressure of water vapor in  $N/m^2$ .

The density of the air is given by

$$\sigma_{air} = \frac{PM}{R^* T} \quad kg/m^3 \quad (2.7.3)$$

where

$R^*$  is the universal gas constant,  $8.31439 \times 10^3 JK^{-1}(kg)^{-1}$ ,

T is the temperature in kelvins (K),

M is the molecular weight, 28.966, and

P is the atmospheric pressure, in  $N/m^2$ .

---

\*Strictly speaking, as noted in Section 2.6, there is a frequency dependence to the water-vapor contribution at frequencies above 10 GHz. In this example, since the water vapor content did not change, the 44 GHz changes are still correct.

\*\*1000 millibars is  $10^5 N/m^2$ .

For the Arizona haboob the following meteorological parameters were measured:

	<u>EXTERNAL</u>	<u>INTERNAL</u>
Atmospheric Pressure, mb	972	972
Temperature, °C (°F)	34.4 (94)	20.6 (69)
Relative Humidity, %	33	81
Visibility, km	~10	~0.4

It will be assumed that the dust density required to produce the ~400-meter visibility is the same as that measured in sandstorms by Schutz and Jaenicke [1974] and given in Table 2.4.1.1 as  $9.13 \times 10^{-4}$  kg/m<sup>3</sup>, even though Lawson [1971] measured a much smaller value of  $4 \times 10^{-5}$  kg/m<sup>3</sup>. Al-Hafid, Gupta, and Buni [1979] estimate  $2 \times 10^{-2}$  kg/m<sup>3</sup> of suspended dust required to produce a 100- to 200-meter visibility. From (2.2.9) this would require an effective radius, of  $r_e = 2.9$  to  $5.9 \times 10^{-4}$  m. Since these represent the maximum size of particles likely to become airborne in a dust storm (at any significant altitude) [see Schutz and Jaenicke, 1974; Ghobrial, Ali, and Hussien, 1978], it seems they made an assumption, as did Chu [1979], that the dust particles are all the same size and equal to the largest observed. This assumption would increase the radio-frequency effects by over one order-of-magnitude; unfortunately, it is wrong.

The value of  $\epsilon$  for sand is that given in Section 2.5,  $\epsilon = 3.36[1 - j0.025]$ ; the value of  $\sigma$  is assumed to be 2600 kg/m<sup>3</sup>. The attenuation can be computed from relations detailed in Section 2 of this report.

The various atmospheric characteristics external and internal to the haboob are detailed in Table 2.7.1. Using the relations in (2.7.1), (2.7.2) and (2.7.3), together with Section 2.3 and other calculations, the effects of the atmospheric changes on N, loss due to oxygen and water vapor, and visibility can be computed. The results are given in Table 2.7.2. Finally, the resultant effects of the dust alone and the atmospheric changes (P, T and humidity) alone are detailed in Table 2.7.3.

TABLE 2.7.1  
EXTERNAL AND INTERNAL CHARACTERISTICS OF A HABOOB OR DUST STORM

<u>CHARACTERISTIC</u>	<u>EXTERNAL</u>	<u>INTERNAL</u>	<u>DIFFERENCE</u>
ATMOSPHERIC PRESSURE, $N/m^2$	$9.72 \times 10^4$	$9.72 \times 10^4$	0
TEMPERATURE, K	307.4	293.6	-13.8
PARTIAL PRESSURE OF WATER VAPOR, $N/m^2$	$1.77 \times 10^3$	$1.94 \times 10^3$	$1.68 \times 10^2$
ATMOSPHERIC DENSITY, $kg/m^3$ (EXCLUDING WATER)	1.1016	1.1534	$+5.18 \times 10^{-2}$
WATER VAPOR DENSITY, $kg/m^3$	$1.37 \times 10^{-2}$	$1.50 \times 10^{-2}$	$1.3 \times 10^{-3}$
DUST DENSITY, $kg/m^3$	0	$9.13 \times 10^{-4}$	$9.13 \times 10^{-4}$

TABLE 2.7.2  
 INDICES OF REFRACTION, PATH LOSSES DUE TO O<sub>2</sub> AND H<sub>2</sub>O, AND VISIBILITY EXTERNAL TO  
 AND INTERNAL TO A HABOOB

<u>EFFECT</u>	<u>EXTERNAL</u>	<u>INTERNAL</u>	<u>DIFFERENCE</u>
R <sub>e</sub> {N <sub>air</sub> }	315.5	341.5	+26
R <sub>e</sub> {N <sub>dust</sub> }	0	0.232	+0.232
I <sub>m</sub> {N <sub>dust</sub> }	0	-4.635x10 <sup>-3</sup>	-4.635x10 <sup>-3</sup>
O <sub>2</sub> and H <sub>2</sub> O Loss at 11 GHz, dB/m	4.6x10 <sup>-5</sup>	5.1x10 <sup>-5</sup>	5x10 <sup>-6</sup>
O <sub>2</sub> and H <sub>2</sub> O Loss at 44 GHz, dB/m	7.4x10 <sup>4</sup>	8.1x10 <sup>-4</sup>	7x10 <sup>-5</sup>
Visibility (R <sub>m</sub> ), km	10	0.35	~30 Fold Reduction

TABLE 2.7.3  
 COMPARISONS OF DENSITY CHANGES AND 11- AND 44-GHz EXCESS PHASE SHIFT AND ATTENUATION  
 CHANGES FROM INSIDE AND OUTSIDE THE ARIZONA HABOOB\*

RESULT	FREQUENCY	DUST COMPONENT		OTHER ATMOSPHERIC COMPONENTS
		ALONE		
CHANGE IN EXCESS	11 GHz	3.06		343
PHASE SHIFT, °/km	44 GHz	12.25		1373
CHANGE IN EXCESS	11 GHz	$9.3 \times 10^{-3}$		$5 \times 10^{-3}$
ATTENUATION, dB/km	44 GHz	$3.7 \times 10^{-2}$		$7 \times 10^{-2}$
CHANGE IN DENSITY kg/m <sup>3</sup>	--	$9.13 \times 10^{-4}$		$5.18 \times 10^{-2}$

\* Comparisons are made for dust alone and atmospheric refractive index alone.



It seems that, aside from a small, direct attenuation, the effects of the dust content of a sandstorm are negligible compared to the other meteorological changes taking place. The change in the density of the air is about 57-times greater than the density of the suspended dust (a similar ratio was noted by Lawson [1971]). The excess phase shifts produced by atmospheric changes are over 100-times greater than those produced by the dust alone. Approximately 65% of the change in attenuation at 11 GHz is due to dust; at 44 GHz the proportion drops to less than 35%.

Finally, how does one account for the 2- to 4-dB reduction in median signal level observed by the Iraqis? It is assumed that the "patchy" character of the haboob air mass coupled with the very large excess phase shifts due to atmospheric density changes can easily produce the 10- to 15-dB deep multipath fading observed. The Nasiriya-Baghdad link stretches 300 km. Therefore, many repeaters will be required. It is likely that only 1 or 2 members will be affected by a single haboob, because the individual "hops" will be about 40 km and storms with diameters much larger than 40 km would be unusual.

It is possible that some of the drop in median signal power occurs because the fade statistics for a signal with unchanged mean value can have a lower median (characteristic, for example, of lognormally distributed signal amplitudes). Rainfall accompanying the storm may also produce some 11 GHz signal-level reductions. However, there is another even more likely mechanism.

If the repeater path lengths are D meters, the first Fresnel-zone radius at midpath is

$$f = \sqrt{\frac{\lambda D}{2}} \quad \text{m} \quad (2.7.4)$$

For normal atmospheric refraction, the effective earth radius can be considered to be 4/3's larger than the physical radius. In order that the first Fresnel zone clear the midpath surface of a smooth 4/3's-earth, 40-km

path at 11 GHz, the terminal elevations must be greater than 46.9 m. For a path passing through a haboob, the lapse rate at low altitudes no longer holds and the effective 4/3's-earth radius reverts to the physical earth radius. (In fact, under certain path conditions the refraction can reverse and the effective earth can be smaller than the physical earth.) As a result, the midpath point no longer clears the earth's surface by 23.36 meters, but only by 15.5 meters.

From Bullington [1957], this effective partial depression of the first Fresnel zone "below ground" gives a loss of about 4 dB over a smooth spherical earth with unity reflection coefficient. The situation in a real-world microwave link is, of course, much more complex. However, the marked changes in atmospheric refractivity accompanying the dust storm would be expected to produce measurable median signal loss, in addition to multipath fading.

Finally, since the late-time dust content of the cloud produced by a near-surface nuclear detonation is comparable to that of a dust-storm, similar comments on atmospheric refractivity can be made. However, in a nuclear detonation the temperatures are so large that very large density changes occur in the atmosphere, amounting to significant fractions of the  $1.225 \text{ kg/m}^3$  density of the standard atmosphere. The resulting changes in refractive index will be many orders-of-magnitude greater than that produced by the entrained dust. Consequently, all effects due to the suspended particulate matter, except near ground zero and in the first 10-30 seconds\*, are totally swamped by gross changes in atmospheric refractive index. (One could make the same statement about the dust raised by a volcanic eruption.)

---

\*Probably only of academic interest to those terminals near enough to ground zero to be concerned.

### III. CONCLUDING REMARKS

Although many investigators have assumed that the suspended dust particles in sandstorms and in the clouds produced by large conventional and nuclear explosions have significant effects on millimeter-wave propagation, such is generally not the case. Only in the case where propagation paths cross close to ground-zero in a large detonation, and even then only in the very early stages of the explosions (first 30 seconds or so), are there likely to be significant effects on radio propagation from suspended particulate matter. Terrestrial microwave links whose paths are intersected by a ground-burst or near-ground detonation might show brief effects. Because of the elevation of the beam in satellite terminals, only those terminals close to ground-zero would show propagation effects; it seems quite likely such terminals will have other, much more significant worries.

The major cause of fading and median signal level reductions in terrestrial paths traversing sandstorms is the significant refractive index changes brought about by the temperature and humidity differentials between the "inside" and "outside" of the sandstorm. In addition, there are significant, small-scale (10 to 20 meters) inhomogeneities in the refractive index inside the storm because of "entrapped" outside air; coupled with the large excess phase changes, such patches make multipath fading very likely on long terrestrial paths. Since a satellite/terminal path would only extend a few kilometers through a storm, such a path is less likely to exhibit multipath fading.

Near the edge of the storm front, some apparent movement of the satellite's radio position might be caused by the large traveling discontinuity in refractive index (due to temperature and humidity differentials). However, the movement is small and would only be important for large, fixed, ground-based apertures at millimeter-wave frequencies with no correction capability for small deviations in apparent satellite position. All of these problems, if they exist, would be noted in any geographic area where such frontal situations occur. Moreover, the

path at 11 GHz, the terminal elevations must be greater than 46.9 m. For a path passing through a haboob, the lapse rate at low altitudes no longer holds and the effective 4/3's-earth radius reverts to the physical earth radius. (In fact, under certain path conditions the refraction can reverse and the effective earth can be smaller than the physical earth.) As a result, the midpath point no longer clears the earth's surface by 23.36 meters, but only by 15.5 meters.

From Bullington [1957], this effective partial depression of the first Fresnel zone "below ground" gives a loss of about 4 dB over a smooth spherical earth with unity reflection coefficient. The situation in a real-world microwave link is, of course, much more complex. However, the marked changes in atmospheric refractivity accompanying the dust storm would be expected to produce measurable median signal loss, in addition to multipath fading.

Finally, since the late-time dust content of the cloud produced by a near-surface nuclear detonation is comparable to that of a dust-storm, similar comments on atmospheric refractivity can be made. However, in a nuclear detonation the temperatures are so large that very large density changes occur in the atmosphere, amounting to significant fractions of the  $1.225 \text{ kg/m}^3$  density of the standard atmosphere. The resulting changes in refractive index will be many orders-of-magnitude greater than that produced by the entrained dust. Consequently, all effects due to the suspended particulate matter, except near ground zero and in the first 10-30 seconds\*, are totally swamped by gross changes in atmospheric refractive index. (One could make the same statement about the dust raised by a volcanic eruption.) If, however, the explosion took place over water, the entrained water would be an important contributor to attenuation and phase shift, particularly at millimeter-wave frequencies.

---

\*Probably only of academic interest to those terminals near enough to ground zero to be concerned.

#### ACKNOWLEDGMENTS

The author is indebted to David J. Frediani, of M.I.T./Lincoln Laboratory whose earlier analyses of sandstorm effects on radio propagation paved the way for this report. Both his analysis and his reference searches proved invaluable. Thanks are also due to Edward A. Bucher of M.I.T./Lincoln Laboratory, who supplied valuable reference material on nuclear and conventional explosion dust generation, to Maj. Leon A. Wittwer of the Atmospheric Effects Division of the Defense Nuclear Agency for commentary and review, and to Maureen E. Bartlett, who typed the drafts and final copy of this manuscript.

## REFERENCES

1. I. Y. Ahmed, and L. J. Auchterlonie, "Microwave Measurements on Dust, Using an Open Resonator," Electronics Lett. 12, pp. 445-446 (19 August 1976).
2. H. T. Al-Hafid, S. C. Gupta, and K. Buni, "Effect of Adverse Sand-Storm Media on Microwave Propagation," Proceedings of National Radio Science Meeting/URSI F.8, p.256 (18-22 June 1979).
3. H. T. Al-Hafid, S. C. Gupta, and M. Ibrahim, "Propagation of Microwaves Under Adverse Sand-Storm Conditions of Iraq," Proceedings of North American Radio Science Meeting/URSI F.5/AP-S, p. 274 (2-6 June 1980).
4. R. A. Bagnold, The Physics of Blown Sand and Desert Dunes, Methuen & Co., Ltd, London (1941).
5. K. Bullington, "Radio Propagation Fundamentals," Bell Sys. Tech. J. 36, pp. 593-626 (May 1957).
6. A. A. Burns, "UHF/SHF Transmission Experiment," Proceedings of the Dice Throw Symposium: 21-23 June 1977, 2, General Electric Company - TEMPO DASIAC (July 1977).
7. A. A. Burns, and P. L. Crawley, "Dice Throw UHF/SHF Transmission Experiment: Volume III - Final Data Reduction and Interpretation," Report No. DNA 4216T-3, S.R.I. International (1 August 1979).
8. R. D. Cadle, Particles in the Atmosphere (McGraw-Hill, New York, 1966).
9. W. S. Chepil, "Sedimentary Characteristics of Dust Storms: III. Composition of Suspended Dust," Amer. J. of Sci 255, pp. 206-213 (March 1957).
10. T. S. Chu, "Effects of Sandstorms on Microwave Propagation," Bell Sys. Tech. J. 58, pp. 549-555 (February 1979).
11. S. I. Ghobrial, I. A. Ali, and H. M. Hussien, "Microwave Attenuation in Sandstorms," Proc. of Inter. Symp. on Ant. and Prop., Sendai, Japan, pp. 447-450 (29-31 August 1978).
12. S. Glasstone, The Effects of Nuclear Weapons - Revised Edition, (U.S. Atomic Energy Commission, April 1962).
13. H. L. Green, and W. R. Lane, Particulate Clouds: Dusts, Smokes and Mists (E. F. & N. Spon, Ltd., London 1957).
14. Handbook of Geophysics - Revised Edition, USAF Air Research and Development Command (MacMillan Company, New York 1961).

REFERENCES (Cont'd)

15. G. B. Hoidale, B. D. Hinds, and R. B. Gomez, "Worldwide Data on Reduced Visibility Due to Airborne Dust," *J. Opt. Soc. Amer.* 67, pp. 1688-1690 (December 1977).
16. S. B. Idso, R. S. Ingram, and J. M. Pritchard, "An American Haboob," *Bull. Amer. Meteor. Soc.* 53, pp. 930-935 (October 1972).
17. C. E. Junge, Advances in Geophysics V. IV, (Academic Press, New York 1957).
18. K. L. Koester, and L. H. Kosowsky, "Millimeter Wave Propagation in Fog," 1971 G-AP International Symposium Digest, pp. 329-332 (22-24 December 1971).
19. T. J. Lawson, "Haboob Structure at Khartoum," *Weather* 26, pp. 105-112 (1971).
20. E. J. McCartney, Optics of the Atmosphere: Scattering by Molecules and Particles (Wiley & Sons, New York 1976).
21. R. P. Rafuse, "Rain-Outage Reduction by Data Storage in EHF SATCOM Systems," Project Report DCA-10, Lincoln Laboratory M.I.T. (25 November 1980).
22. Reference Data for Radio Engineers - Fifth Edition, Howard W. Sams, Inc., Division of ITT, Indianapolis (1968).
23. L. Schutz, and R. Jaenicke, "Particle Number and Mass Distributions above  $10^{-4}$  cm Radius in Sand and Aerosol of the Sahara Desert," *Jour. App. Meteor.* 13, pp. 863-870 (December 1974).
24. M. I. Skolnik, Radar Handbook (McGraw-Hill, New York 1970).
25. J. A. Stratton, Electromagnetic Theory (McGraw-Hill, New York 1941).
26. J. H. Thompson, "Dust Cloud Modeling and Propagation Effects for Radar and Communications Codes," Report No. DNA 4697T, General Electric Company-TEMPO (1 November 1978) DDC A071368.
27. H. C. Van DeHulst, Light Scattering by Small Particles (Wiley & Sons, New York 1957).

UNCLASSIFIED

SECURITY CLASSIFICATION OF THIS PAGE (When Data Entered)

REPORT DOCUMENTATION PAGE		READ INSTRUCTIONS BEFORE COMPLETING FORM
1. REPORT NUMBER ESD-TR-81-290	2. GOVT ACCESSION NO. AD-A1094190	3. RECIPIENT'S CATALOG NUMBER
4. TITLE (and Subtitle) Effects of Sandstorms and Explosion-Generated Atmospheric Dust on Radio Propagation		5. TYPE OF REPORT & PERIOD COVERED Project Report
		6. PERFORMING ORG. REPORT NUMBER Project Report DCA-16
7. AUTHOR(s) Robert P. Rafuse		8. CONTRACT OR GRANT NUMBER(s) F19628-80-C-0002
9. PERFORMING ORGANIZATION NAME AND ADDRESS Lincoln Laboratory, M. I. T. P. O. Box 73 Lexington, MA 02173		10. PROGRAM ELEMENT, PROJECT, TASK AREA & WORK UNIT NUMBERS Program Element No. 33126K
11. CONTROLLING OFFICE NAME AND ADDRESS Defense Communications Agency 8th Street and So. Courthouse Road Arlington, VA 22204		12. REPORT DATE 10 November 1981
		13. NUMBER OF PAGES 66
14. MONITORING AGENCY NAME & ADDRESS (if different from Controlling Office) Electronic Systems Division Hanscom AFB Bedford, MA 01731		15. SECURITY CLASS. (of this report) Unclassified
		15a. DECLASSIFICATION DOWNGRADING SCHEDULE
16. DISTRIBUTION STATEMENT (of this Report)  Approved for public release; distribution unlimited.		
17. DISTRIBUTION STATEMENT (of the abstract entered in Block 20, if different from Report)		
18. SUPPLEMENTARY NOTES  None		
19. KEY WORDS (Continue on reverse side if necessary and identify by block number)  explosion-generated dust      sandstorms/dust storms      SHF/EHF propagation through dust		
20. ABSTRACT (Continue on reverse side if necessary and identify by block number)  The effect of man-made and natural airborne dust on SHF and EHF propagation is investigated. It is found that atmospheric pressure, temperature and humidity changes, and not suspended dust, are the major causes of observed fading and attenuation of rf signals transiting the dust clouds.		

DD FORM 1473 EDITION OF 1 NOV 65 IS OBSOLETE  
1 JAN 73

UNCLASSIFIED

SECURITY CLASSIFICATION OF THIS PAGE (When Data Entered)



ESD-TR-81-290

ERRATA SHEET

for

PROJECT REPORT DCA-16

The author of Project Report DCA-16 (R. P. Rafuse, "Effects of Sandstorms and Explosion-Generated Atmospheric Dust on Radio Propagation, 10 November 1981) has discovered that pages 51 and 53 should be replaced with the attached pages.

The views and conclusions contained in this document are those of the contractor and should not be interpreted as necessarily representing the official policies, either expressed or implied, of the United States Government.

The Public Affairs Office has reviewed this report, and it is releasable to the National Technical Information Service, where it will be available to the general public, including foreign nationals.

Approved for public release; distribution unlimited.

23 December 1981

Publications  
M.I.T. Lincoln Laboratory  
P. O. Box 73  
Lexington, MA 02173

path at 11 GHz, the terminal elevations must be greater than 46.9 m. For a path passing through a haboob, the lapse rate at low altitudes no longer holds and the effective 4/3's-earth radius reverts to the physical earth radius. (In fact, under certain path conditions the refraction can reverse and the effective earth can be smaller than the physical earth.) As a result, the midpath point no longer clears the earth's surface by 23.36 meters, but only by 15.5 meters.

From Bullington [1957], this effective partial depression of the first Fresnel zone "below ground" gives a loss of about 4 dB over a smooth spherical earth with unity reflection coefficient. The situation in a real-world microwave link is, of course, much more complex. However, the marked changes in atmospheric refractivity accompanying the dust storm would be expected to produce measurable median signal loss, in addition to multipath fading.

Finally, since the late-time dust content of the cloud produced by a near-surface nuclear detonation is comparable to that of a dust-storm, similar comments on atmospheric refractivity can be made. However, in a nuclear detonation the temperatures are so large that very large density changes occur in the atmosphere, amounting to significant fractions of the  $1.225 \text{ kg/m}^3$  density of the standard atmosphere. The resulting changes in refractive index will be many orders-of-magnitude greater than that produced by the entrained dust. Consequently, all effects due to the suspended particulate matter, except near ground zero and in the first 10-30 seconds\*, are totally swamped by gross changes in atmospheric refractive index. (One could make the same statement about the dust raised by a volcanic eruption.) If, however, the explosion took place over water, the entrained water would be an important contributor to attenuation and phase shift, particularly at millimeter-wave frequencies.

---

\*Probably only of academic interest to those terminals near enough to ground zero to be concerned.

refractive-index effects (other than dust-generated) are substantially frequency independent and, therefore, present equivalent problems at any frequency (aside from a small frequency dependence caused by the relationship of the Fresnel zone size to the scale of turbulence). The sand and dust suspended in some of the storms are "effects", not "causes", and serve a useful purpose for meteorologists by acting as a convenient visual "tracer" for the storm.

There are strong indications that the probability density distribution for suspended-particle radii is a strong function of altitude, with a rapid decrease in the population of larger particles in only a few meters of elevation. Since the effect of such an altitude dependence on the value of  $r^3$  is much more pronounced than the effect on  $r^2$ , the changes in such optical measures as visibility are minimal, but radio-frequency effects are more pronounced. Essentially, such a density gradient means that near-surface terrestrial links would show the most effect from suspended dust, while elevated sites or slant paths, such as those in SATCOM systems, would be less affected.

Finally, even at frequencies as high as 44 GHz, the total contribution of the dust in a dust storm or sandstorm to the attenuation of a radio signal is of the same order as that produced by oxygen and water-vapor changes. For slant paths the relative contribution of the dust would be reduced further by the altitude density gradient. In a large nuclear explosion, the rain which often forms on the smaller nuclei late in the history of the event would produce much more attenuation at millimeter waves than would the suspended particulate matter.